QUEST RJ

ISSN 1665-8607
Bi - Annual

QUAID-E-AWAM UNIVERSITY RESEARCH JOURNAL

OF ENGINEERING, SCIENCE & TECHNOLOGY

MISSION STATEMENT OF QUEST

"To Provide quality and state-of-the art education (coursework, practical training and research) in prescribed branches of Engineering and Science to the enrolled students in order to make them better professionals and better human being; so that they become capable of contributing amicably towards national development".

Volume 9 No. 2 JUL-DEC- 2010

Bi-annual: ISSN 1665-8607

Quaid -e- Awam University Research Journal of Engineering, Science & Technology

EDITORIAL BOARD

ANNUAL SUBSCRIPTION .....Rs. 200.00 (INLAND). US$ 20.00 (FOREIGN, SURFACE MAIL)
SINGLE ISSUE .....Rs. 100.00 (INLAND). US$ 10.00 (FOREIGN, SURFACE MAIL)

The Bi-Annual Quaid-e-Awam University Research Journal of Engineering, Science & Technology, Shall be supplied free of cost in exchange of Research Journal (s) from other Universities / Institutions and Research Centres.

ISSN 1665 - 8607

ACKNOWLEDGMENT

The members of Editorial Board, Quaid-e-Awam University Research Journal of Engineering, Science & Technology are grateful for valuable and critical suggestions on various Research Paper (s) sent to following Researchers / Experts for Volume 9 No. 2 July - December 2010 Issue. The members also appreciate the Referees / Experts for sharing their knowledge and expertise towards improvement of standard of this research Journal.

1. **Professor Li JinLin**
   School of Management & Economics,
   Beijing Institute of Technology (BIT), P.R. CHINA.

2. **Dr. Muhammad Idress**
   Department of Electrical Engineering,
   City University, Peshawar.

3. **Dr. Irfan Jaffar**
   NU-FAST, Islamabad.

4. **Dr. Rana Muhammad Ramzan**
   Department of Mathematics,
   The Islamic University Bhawalpur.

5. **Prof. Dr. Bhawani Shankar**
   Department of Electronic & Bio Medical Engineering,
   MUET, Jamshoro.

6. **Prof. Dr. Mukhtiar Ali Unar**
   Department of Computer System Engineering,
   MUET, Jamshoro.

7. **Prof. Dr. G . Bux Khaskali**
   Department of Civil Engineering,
   MUET, Jamshoro.

8. **Prof. Gul Hassan Memon**
   Department of Civil Engineering,
   MUET, Jamshoro.

9. **Prof. Dr. Rasool Bux Mahar**
   Department of Environmental Engineering
   MUET, Jamshoro.

10. **Dr. Najama Memon**
    University of Sindh, Jamshoro.

11. **Prof. Dr. Attaullah Khawaja**
    Department of Electronic Engineering,
    NED, Karachi.

12. **Prof. Dr. Abdul Hameed Memon**
    Department of Mechanical Engineering,
    QUEST, N/SHAH.

13. **Prof. Dr. Abdul Sattar Jamali**
    Department of Mechanical Engineering,
    QUEST, N/SHAH.

14. **Prof. Dr. Altaf Hussain Rajpar**
    Department of Mechanical Engineering,
    QUEST, N/SHAH.

A STUDY ON THE TRANSFORMATION OF VARIOUS MATRICES OF S. G IRON INTO AUSTEMPERED DUCTILE IRON

M. Ajmal*, M. Y. Anwar**, R. Adeel***

ABSTRACT

Austempered Ductile Iron (ADI) can be made by the austempering of spheroidal graphite (S. G) iron. Austempering changes the matrix nature of ferrite or pearlite to ausferrite (austempered) plus retained austenite. The austempered matrix has better mechanical properties as compared to ferritic or pearlitic matrix of S.G iron. Therefore, austempered ductile iron can be of great importance in our agricultural industry. In the present work, commercially used grades of S. G iron with ferritic matrix (dented by A) and pearlitic matrix (denoted by B) were austempered to produce a tempered austenite matrix of ductile iron. Both S.G irons (A) and (B) were austenitised to 950 °C. Ferritic matrix S. G iron (A) was austempered to 250 °C and 300 °C for 15, 30, 45, and 60 minutes, respectively. Whereas pearlitic matrix S. G iron (B) was austempered at 300 °C and 400 °C for 15, 30, 45 and 60 minute, respectively. Austempering of S. G iron with ferritic matrix at 250 °C and 300 °C shows almost same hardness. However, austempering of S.G iron of pearlitic matrix at 250 °C shows higher hardness values at all holding times as compared to austempering at 400 °C. It can be concluded that the S. G iron(A) of ferrite matrix is less responding to austempering as compared to the pearlitic matrix (B). Thus, better mechanical properties such as high hardness/wear resistance can be achieved by using S. G iron (B) of pearlitic matrix less responding to austempering as compared to the pearlitic matrix (B). Thus, better mechanical properties such as high hardness/wear resistance can be achieved by using S. G iron (B) of pearlitic matrix.

1. INTRODUCTION

It is well known that heat treatment cycle for austempering of ductile iron consists of austenitising it between 850- 950 °C, followed by fast quenching into a low temperature and held isothermally in the austempering range 200-400 °C for a specified length of time to complete the transformation and then air cool/quench [1, 2]. The processing window for austempring temperature was also determined on the basis of the mechanical properties as required by ASTM A897M-03 standards [3]. During the austenitisation of ductile iron carbon from the nodules may dissolves in the austenite to attain its equilibrium concentration. This austenite is then quenched rapidly at slightly above the martensite start transformation temperature to avoid the formation of pearlite/ferrite [4].

S. G iron is austenitised either using a high temperature salt bath or a controlled atmosphere furnace. It is established by many workers [4-6] that initial austenitising time and temperature (850 – 950 °C) must be controlled to form fine grain austenite and uniform carbon contents in the matrix.

It has been observed [1, 5, 6] that during austempering ferrite is nucleated and grows from the parent austenite. At the same time the carbon rejected from the growing ferrite diffuses into surrounding austenite enriching the carbon content of austenite rather than forming the carbide.

Many researchers [1, 5, 6] suggested that the austempering reaction in ductile iron over the temperature range 200-400 °C occurs in two stages. During 1st stage transformation starts by the nucleation of bainitic ferrite at the inter phase and grain boundaries, and then grows into austenite. This is associated with the carbon rejection from growing ferrite plates into the surrounding austenite. The carbon enrichment of austenite occurs during holding time and enrichment of austenite takes place up to 1.8-2.2 % C. The structure of first stage is called upper bainite which consists of relatively coarse bainitic plates plus retained austenite in the matrix. This product is also known as upper ausferrite.

During 2nd stage with extended austempering period, high carbon stable austenite further decomposes into more stable fine bainitic ferrite and carbide, nominally called

* Department of Metallurgical and Materials Engineering, UET, Lahore-Pakistan, E-mail: mohammad_ajmal@hotmail.com
** Department of Metallurgical and Materials Engineering, UET, Lahore-Pakistan
***Department of Metallurgical and Materials Engineering, UET, Lahore-Pakistan

ISSN 1665-8607

lower bainite or lower ausferrite. It has been observed by many workers [6, 7] that the undesirable 2nd stage of austempering reaction, where austenite decomposes to form ferrite and carbide, occurs much more readily when austempering at high transformation temperatures.
Some new terminologies are being introduced to illustrate the above mentioned differences in austempering reaction at low and high transformation temperatures [1, 7].

The austenite transformed at higher austempering temperatures which can result in the formation of carbide free ferrite and stabilized austenite is called as "austempered ductile iron". The fine ferrite, carbide and stabilized austenite structure, formed at lower austempering transformation temperatures, is known as "austempered/bainitic ductile iron". It is reported [4] that the structures obtained from austempering of ductile iron and steel are quite different; therefore, they are appropriately termed as ausferrite and bainite, respectively. It is well known that austempered ductile irons are used where both high toughness and strength is required, while austempered bainitic ductile irons are employed when highest strength and wear resistance is needed.

S. G iron is mainly employed for the production of parts which are mostly utilized in automobile and agricultural industries, where wear resistance/ high hardness and toughness are the basic requirements. These parts of S. G iron are mostly produced using gas fired furnaces. This S. G iron is not as clean as is required for the austempering [8]. However, in the present work an effort has been made to improve the properties particularly hardness of this indigenously produced S. G iron by austempering.

2. EXPERIMENTAL WORK

Two types of S. G irons, produced by employing a gas fired furnace, were selected for the present study. The compositions of S. G iron "A" and S. G "B" are given in the Table 1. Both the S. G irons were austenitised at 950 °C and then austempered at two different temperatures for a various length of times. Individual temperature and time span for austempering of both S. G irons 'A' and 'B' is shown in Figures 1 and 2, respectively

Table 1: Composition of S. G irons A and B.

Elements	% C	% Si	% Mn	% P	% S
S.G. Iron "A"	3.4	1.85	0.24	0.004	0.005
S.G. Iron "B"	3.7	2.5	0.35	0.004	0.004

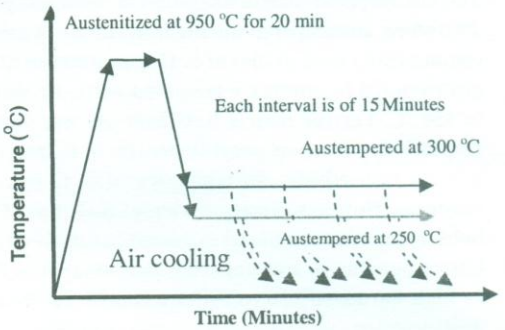

Figure 1: Schematic representation of Austempering of S.G Iron 'A' at various temperatures and times.

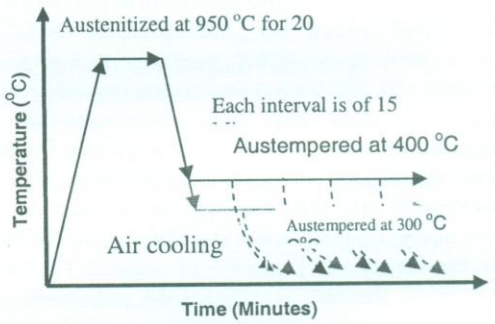

Figure 2: Schematic representation of Austempering of S.G Iron 'B' at various temperatures and times.

Cubic shaped samples of S. G iron "A" having dimensions approximately 1.5 cm were austerities in a muffle furnace at 950 °C for 20 minutes. One of the austenitised samples at 950 °C for 20 minutes was taken out from the furnace and immediately quenched in the water. Another austenitised sample was held in air for 10 seconds (which was the time taken in moving samples from one furnace to another furnace) before quenching in water. Remaining austenitised samples were immediately transferred to other muffle furnaces which were maintained at 300 °C and 250 °C, respectively, for

austempering. At these temperatures, austempering was carried out for 15, 30, 45 and 60 minutes, respectively and then these austempered samples were quenched in water.

Various samples of S.G iron "B" having dimensions similar to S. G iron "A" were also austenitised at 950 °C for 20 minutes. One of the austenitised specimen was taken out from the furnace and immediately quenched in the water. Remaining samples were austempered in muffle furnaces at 400 °C and 300 °C for 15, 30, 45, 60 minutes, respectively and then quenched in water. The temperatures of the furnaces were monitored by Chromel/Alumel (T1/T2) thermocouple.

Prior examination had shown that depth of the surface layer damaged by decarburization was less than 0.5 mm. Therefore, these heat treated specimens were ground to remove 1mm of material. The micro structural studies of polished and etched samples (2% nital) were carried out using an Olympus PME 3 inverted Metallurgical Microscope. Hardness values of all heat-treated and as received samples were measured by using a Brinell hardness testing machine.

3. RESULTS & DISCUSSIONS

The microstructure of a sample of as cast S. G iron "A" containing approximately 80% ferrite is shown in Figure 3. It can be seen in Figure 3 that graphite nodules are surrounded by ferrite rings and dark areas other than nodules in the matrix are pearlite .This type of structure is called a bull's eye structure [9].

Figure 4, is a representative microstructure of as cast S. G iron "B" which shows more pearlitic areas (approximately 80%) in the matrix as compared to S.G iron "A". This more pearlitic area in the microstructure of S. G iron "B" as compared to "A" may be due to more carbon in S. G. iron "B". Ferrite rings around the nodules can also be observed in the Figure 4. However, the size of the ferrite rings in case of S. G iron "B" is smaller as compared to S.G iron "A".

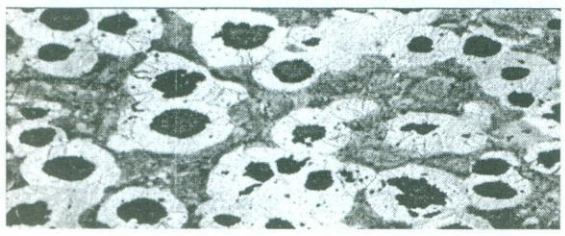

100X

Figure 3: As cast S.G iron "A".

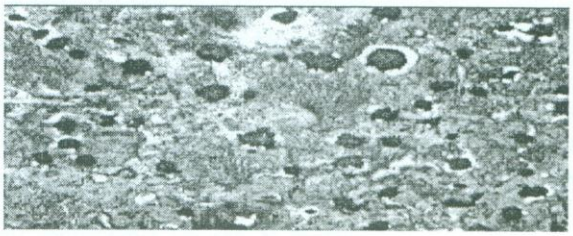

100X

Figure 4: As cast S.G iron "B".

The microstructure of the S. G iron "A" austenitized at 950 °C for 20 minutes and quenched in water is shown in Figure 5. The matrix has been converted to austenite when heated at 950 °C and quenching of that austenite transforms it into martensite. The highest hardness number of this sample also verifies that during quenching austenite matrix has transformed in to harder product i.e. martensite.

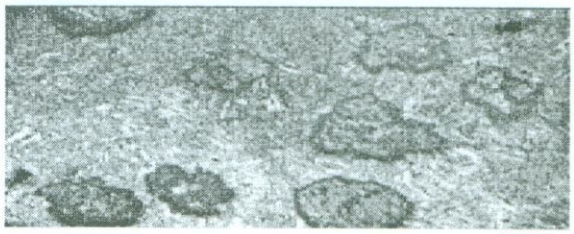

250X

Figure 5: Austenitised at 950 °C and quenched in water.

Figure 6 shows the microstructure of S. G iron "A" austenitized at 950 °C and held in air for 10 seconds (the time required for shifting the sample to another furnace for austempering) and then quenched. It can be seen that whole of the austenite transformed to martensite. Thus, it can be concluded that the transferring time from austenitization furnace to austempering furnace does not allow the transformation of austenite to softer products (ferrite or pearli

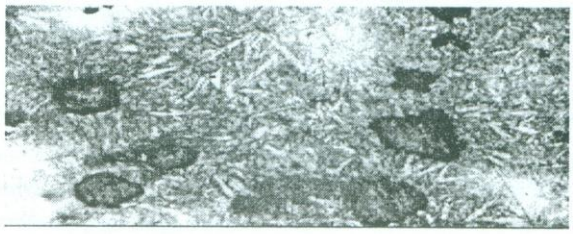

250X

Figure 6: Austenitised at 950 °C held in air for 10 seconds and quenche

ISSN 1665-8607

The microstructure of S. G iron "A" austenitised at 950 °C for 20 minutes and austempered at 250 °C for 15 minutes shows almost complete transformation to ausferrite, i.e. an intermediate phase between pearlite and martensite Figure 7. Similar microstructure (ausferrite) after austempring was produced by some other workers [10, 11]. The hardness values of the specimens as cast, quenched and asutempered at various temperature for different times are given in **Table** 2. This shows that hardness values of as cast S. G iron is BHN 172 whereas hardness of the quenched sample is BHN 440. The S.G iron "A" austenitized at 950 °C for 20 minutes and austempered at 250 °C for 15 minutes shows hardness BHN 265 .Which is in between the hardness values of as cast and quenched samples. The comparison of hardness values as mentioned above also indicates that the austempering transformation, i.e., (ausferrite) is an intermediate phase between pearlite and martensite.

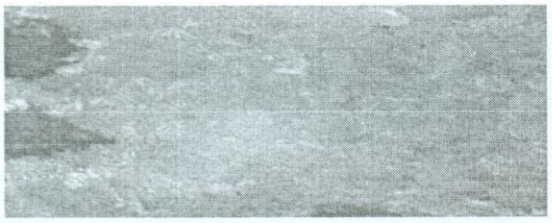

400X

Figure 7: Austempered at 250 °C for 15 minutes "A".

Table 2: Brinell Hardness Number (BHN) for S. G iron "A".

Condition	BHN	Austempered at 300 °C		Austempered at 250 °C	
		Time (Min)	BHN	Time (Min)	BHN
As Cast	172 ± 1.4	15	265 ± 1.5	15	265 ± 1.5
Austenitised and Water Quenched	440 ± 2.3	30	240 ± 1.4	30	231 ± 1.7
		45	249 ± 1.7	45	249 ± 1.5
		60	239 ± 1.3	60	244 ± 1.6

The microstructure of S.G iron "B" austenitised at 950 °C for 20 minutes and austempered at 400 °C for 15 minutes is shown in Figure 8. This Figure shows that the whole matrix has transformed to ausferrite. The same material (S. G. Iron B) was also used for austempering by another worker [12]. Figures 9 (a) and (b) are SEM microstructures of austenitised specimens at 900 °C for 2 hours and austempered at 300 °C for one hour [12]. These microstructures verified that this indigenously produced S. G iron has transformed to ausferri.

400 X

Figure 8: Austempered at 400 °C for 15 minutes "B"

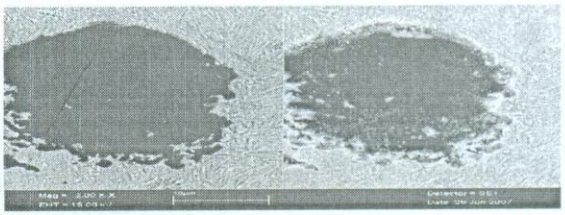

Figure 9 (a): SEM micrograph of ADI showing carbon nodules, right: secondary electron image and left: backscattered image, S. G iron "B" [12].

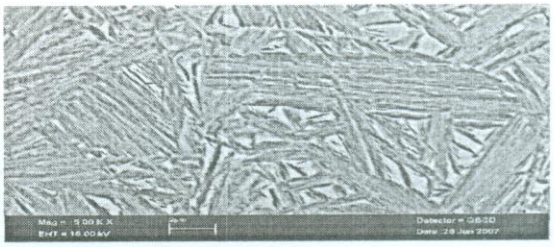

Figure 9 (b): SEM micrograph of bainite sheaves with retained austenite, S. G iron "B" [12].

The hardness of as received and heat treated samples of S. G iron "A" and "B" are given in Tables 2 and 3. It can be seen in Table 2 that S. G iron "A" which was austempered at 250 °C and 300 °C indicates almost same values of hardness at all holding times. The hardness of austempered S. G iron of similar composition and microstructure as of S.G. iron "A" produced at 400°C were measured by Ajmal et. al [13]. It can be observed that that hardness values of ADI produced by Ajmal et. al at 400 °C were almost similar to the hardness of ADI produced by austempering of S. G iron "A" at 250° C and 300° C in present experimentations.

ISSN 1665-8607

Table 3: Brinell Hardness Number (BHN) for S. G iron "B".

Condition	BHN	Austempered at 400 °C		Austempered at 300 °C	
As Cast	199 ± 1.5	Time (Min)	BHN	Time (Min)	BH N
		15	249 ± 1.7	15	265 ± 1.5
Austenitised and Water Quenched	454 ± 2.5	30	240 ± 1.5	30	254 ± 1.6
		45	270 ± 1.4	45	283 ± 1.7
		60	254 ± 1.7	60	249 ± 1.5

The hardness values of S. G iron "B", austempered at 400 °C and 300 °C, are higher than the S. G iron "A" at all holding times, Table 3. It was also observed that higher values of hardness can be achieved if the S. G iron "B" is austempered at 300 °C for 45 minutes. This higher value of hardness of S. G iron "B" austempering at lower temperature, i.e., 300 °C for 45 minutes has been also verified by many workers [10, 11, 13].

4. CONCLUSIONS

1. Austempering of S. G iron "A" at 300 °C and 250 °C shows almost same values of hardness.
2. Austempering of S. G iron "B" at 300 °C yields higher values of hardness at all holding times as compared to austempering at 400 °C.
3. Maximum hardness was achieved in S. G iron "B" austempered at 300 °C for 45 minutes.

REFERENCES

1. R. Elliot, "Cast Iron Technology", Butterworth & Co. Ltd., New York, 1988.
2. O. Erić, et. al., "Determination of Processing Window for ADI Materials Alloyed With Copper", Association of Metallurgical Engineers of Serbia, MJoM , Vol. 16, No.2, pp. 91-102, 2010.
3. M. Erdogan, V. Kilicli, and B. Demir, "Transformation Characteristics of Ductile Iron Austempered from Intercritical Austenitizing Temperature Ranges", J. Mater. Sci., Vol. 44, No.5, pp. 1394–1403, 2009..
4. H. K. D. H. Bhadeshia, et. al.,,"Stress induced transformation to bainite in Fe–Cr–Mo–C pressure vessel steel", Materials Science and Technology, Volume 7, Number 8, pp. 686-698, 1991.
5. H. K. D. H. Bhadeshia, "Bainite in Steels". The institute of Materials, London, pp. 117–121, 1992.
6. N. Darwish and R. Elliot, "Austempering of low manganese ductile irons", Materials Science and Technology, Vol. 9, pp. 572-585, 1993.
7. H. Bayati. and R. Elliott, "Austempering process in manganese alloyed ductile cast iron", Materials Science and Technology, Vol. 11, pp. 118-129, 1995.
8. C. K. Lin and J. Y. Wei, "High-Cycle Fatigue of Austempered Ductile Irons in Various-Sized Y-Block Castings", Materials Transaction, JIM, Vol. 38. No. 8, pp. 682-691, 1997.
9. H. K. D. H. Bhadeshia and D. V. Edmonds, "The Mechanism of Bainite Formation in Steel", Acta Metallurgica, Vol. 28, pp. 1265-1273, 1980.
10. R. C. Thomson, J. S. James and D. C, Putman, "Modelling microstructural evolution and mechanical properties of austempered ductile iron", Materials Science and Technology, Vol. 16, pp. 1412-1419, 2000.
11. R. Kazerooni, A. Nazarboland and R. Elliott , "Use of austenitising temperature in control of austempering of an Mn-Mo-Cu alloyed ductile iron", Materials Science and Technology, Vol. 13, No. 12, pp. 1007-1015, 1997.
12. A. Gulzar, et.al., "Microstructure evolution during surface alloying of ductile iron and austempered ductile iron by electron beam melting", Applied Surface Science, Vol. 255, Issue 20, , PP. 8527-8532, 2009.
13. M. Ajmal and F. Nazir, "Mechanical properties of austempered ductile iron austenitised at different temperatures", Advanced Materials-2005, Dr. A. Q. Khan Research Laboratories, Pakistan, pp 321-324, 2005.

OPTIMAL HOMOTOPY ASYMPTOTIC METHOD FOR SOLVING SIXTH-ORDER BOUNDARY VALUE PROBLEMS

Amjed Javed*, Nisar Ahmed Memon**, Shaukat Iqbal***

ABSTRACT

In this paper, a trusty method-optimal homotopy asymptotic method (OHAM) is applied to solve sixth order nonlinear boundary value problems. To demonstrate the capability, viability and practical usefulness of the method, Computational results of two test problems are presented. It is observed that exact solutions are in absolute conformity with the results of OHAM. It is also examined that the method is quite powerful in handling such kind of problems and easy in implementation.

Keywords: Optimal homotopy asymptotic method; nonlinear boundary value problems; convergence of error.

1. INTRODUCTION

Scientific investigations and modeling of external layers (the stable layers bounding the narrow convecting layers) of A-type stars in astrophysics construct sixth-order boundary value problems (BVPs) [1-2]. Sixth order equations may also emerge when dynamo action in stars is being modeled [3]. Moreover, sixth-order equations also appear when the ordinary convection instability due to rotation by heating of an infinite horizontal layer of fluid is being modeled [4]. Several attempts have been made so for to solve sixth order boundary value problems both numerically and non-numerically [5-12].

Motivated and inspired by the ongoing research work, OHAM [13-17] is experimented to approximate sixth-order nonlinear boundary value problems. Marinca et al. [13] proposed this method: Optimal Homotopy Asymptotic Method (OHAM). Integrated convergence criteria and flexibility in application are the advantages of OHAM. Marinca et al. [14-16] and Iqbal et al. [17], in sequence of their research work, have proved usefulness, efficiency, generalization and reliability of the method.

The objective of this presentation is to elucidate that the OHAM [13-17] is inherently powerful and tenders a reasonable/reliable solution to nonlinear sixth order boundary value problems.

2. OHAM [13-17] FORMULATION

By definition of optimal homotopy asymptotic method [13-17] the general expression for differential equation can be written as:

$$B(v(x)) + g(x) = 0, \quad x \in \Omega, \tag{1}$$

Ω is domain. Now, $B(v) = L(v) + N(v)$. is obtained by decomposing equation (1) According to OHAM [13-17], one can construct an optimal homotopy $\psi(y;p)$: $\Omega \times [0,1] \to \square$ which satisfies:

$$(1-p)\{L(\psi(x;p)) + g(x)\} - H(p)\{B(\psi(x;p)) + g(x)\} = 0, \tag{2}$$

where $p \in [0,1]$ is an embedding parameter, $H(p) = pC_1 + p^2C_2 + \ldots$ is a nonzero auxiliary function for $p \neq 0$, $H(0) = 0$, where $C_1, C_2, \ldots$ are constants to be determined. Equation (2) is called optimal homotopy equation. To get an approximate solution, we expand $\psi(x;p,C_i)$ in Taylor's series about p in the following manner, $\psi(x;p,C_i) = v_0(x) + \sum_{k=1}^{\infty} v_k(x;C_i)\, p^k, \quad i = 1,2,\ldots$ (3)

It has been examined that the convergence of the series equation (3) depends upon the auxiliary constants $C_1, C_2, \ldots$. If it is convergent at $p = 1$, one has:

$$\underline{v}(x;C_i) = v_0(x) + \sum_{k\geq 1} v_k(x;C_i) \tag{4}$$

By putting equation (4) into equation (1), one can get the following expression for residual:

$$R(x;C_i) = L(\underline{v}(x;C_i)) + g(x) + N(\underline{v}(x;C_i)) \tag{5}$$

If $R(x;C_i) = 0$, then $\underline{v}(x;C_i)$ will be the exact solution. Generally it doesn't happen, especially in nonlinear

* Centre for Advance Studies in Engineering, 19-Attaturk Avenue, Islamabad, Pakistan, Email: amjedch.ppn@gmail.com
** Department of Computer Systems Engineering, QUEST, Nawabshah, Pakistan, Email: nisar@quest.edu.pk
*** Theoretical Plasma Physics Division, PINSTECH, Nilore, Islamabd, Pakistan, Email:shaukat.iqbal.k@gmail.com

problems. For the determinations of auxiliary constants, $C_i, i = 1,2,...,m$, one can see the [13-17].

3. APPLICATION OF OHAM [13-17] TO NONLINEAR DIFFERENTIAL EQUATIONS

In this section, the method described in section 2 is tested on the subsequent nonlinear problems of sixth order from the numerical literature [12], the absolute errors are tabulated to see the convergence.

Example.1: Consider the following homogeneous non-linear boundary value problem [12] of sixth order:

$$y^{(6)}(x) - e^{-x} y^2(x) = 0, \quad 0 < x < 1 \tag{6}$$

Subject to the boundary conditions

$y(0) = 1, y''(0) = 1, y''''(0) = 1, y(1) = e, y''(1) = e, y''''(1) = e$. The exact solution of the equation (6) is, $y(x) = e^x$

OHAM formulation described in section 2 leads to the following expression

$$L(\psi(x,p)) = \psi^{(6)}(x,p) \tag{7}$$

$$N(\psi(x;p)) = -e^{-x}\psi^2(x;p) \tag{8}$$

The boundary conditions are:

$$\left.\begin{aligned} &\psi(0;p) = 1, \psi''(0;p) = 1, \psi''''(0;p) = 1 \\ &\psi(1;p) = e, \psi''(1;p) = e, \psi''''(1;p) = e \end{aligned}\right] \tag{9}$$

This generates a series of problems: zeroth order and, first order problems are defined as:

$$y_0^{(6)}(x) = \begin{cases} 0; \\ y_0(0) = 1,\ y_0''(0) = 1,\ y_0''''(0) = 1, \text{ and} \\ y_0(1) = e,\ y_0''(1) = e \text{ and } y_0''''(1) = e \end{cases} \tag{10}$$

$$y_1^{(6)}(x) = \begin{cases} (1 + C_1)\, y_0^{(6)}(x) - e^{-x} C_1 y_0^{\,2}; \\ y_1(0) = 0,\ y_1''(0) = 0, y_1''''(0) = 0, \text{ and} \\ y_1(1) = 0, y_1''(1) = 0 \text{ and } y_1''''(1) = 0 \end{cases} \tag{11}$$

Now, to find y_0 and y_1, one can solve equations (10)-(11) and it will construct the solution for $y(x;p,C_i)$ that allows $p \to 1$ to get $y(x;C_i)$.

Zeroth-order solution: From equation (10), one can get the zeroth-order solution as:

$$y_0(x) = \frac{1}{360}\begin{pmatrix} 360 - 472x + 307ex + 180x^2 - 80x^3 \\ +50ex^3 + 15x^4 - 3x^5 + 3ex^5 \end{pmatrix} \tag{12}$$

First-order solution: By using (12) in equation (11) and applying the boundary conditions, we will find first-order solution as:

$$\begin{aligned} &y_1(x) = \\ &-\frac{e^{-1-x}C_1}{7776000}(-e^x x\ (6795365003983 \\ &+115442736110x^2 + 247124187x^4) + 96e^{1+x} \\ &(-36989233080 + 233225910724x - 5202735x^4 \\ &+4051726500x^3 + 9032451x^5 - 1687813900x^2) \\ &-96e^{2+x}(-102828221760 + 241437311339x \\ &-16223970x^4 + 4209613470x^3 + 9551301x^5 \\ &-4925698100x^2) + e^{3+x}(-6911054864280 \\ &+7142928833248x - 1235620935x^4 \\ &+117913977980x^3 + 247124187x^5 \\ &-348799450200x^2) + 60e(59182772928 + 9x^{10} \\ &+39868689408x + 12977805184x^2 + 257160x^7 \\ &+2703806400x^3 + 402060880x^4 + 44969712x^5 \\ &+3872752x^6 + 12855x^8 + 450x^9) - 120e^2 \\ &(82262577408 + 54802698288x + 495x^9 + 9x^{10} \\ &+17611968064x^2 + 3615042720x^3 + 312270x^7 \\ &+528213520x^4 + 57852147x^5 + 4856077x^6 \\ &+14970x^8) + 60e^3(115184247738 + 17310x^8 \\ &+75793954668\,x + 24015154969x^2 + 540x^9 \\ &+6072502x^6 + 4848961440x^3 + 694959760x^4 \\ &+74385432x^5 + 377280x^7 + 9x^{10})) \end{aligned} \tag{13}$$

Now, by adding zeroth-order and first-order solutions, and other higher order solutions if certainly essential, one can get:

$$y(x) = y_0(x) + y_1(x) + \ldots, \tag{14}$$

For the calculations of the constants C_1, using the procedure pointed out in [13-17], one can get $C_1 = -0.00011990488216293872$. By using the value

of C_1 , one can get solution as:

$$y(x) = e^{-1-x}(0.04352366775542985e^{x}(x - 4.520466980509181)(37.422978420610626 + x^2 - 6.967578063124352x)(157.79799749880002 + x^2 + 8.893905255518462x) + 6682787490319201\times10^{-8} (16311203888274432 + 39190297702026804x + x2) \quad (15)$$
$$(123.69350146498759 + 10.794468840297462x + x^2)$$
$$(103.85294977471929 + 14.970160704404137x + x^2)$$
$$(93.48452797230581 + 17.474622927154154x + x^2)$$
$$(88.96401939582806 + 18.66148482663482x + x^2))$$

This is the approximate solution and comparison with the exact solution is given below in Table 1. This reveals that OHAM [13-17] yields precise results at low order of approximation. Thus one can escape from lengthy and complex calculations.

Example.2: Consider the following homogeneous non-linear boundary value problem [12] of sixth order:

$$y^{(6)}(x) - e^{x}y^{2}(x) = 0, \quad 0 < x < 1 \qquad (16)$$

Subject to the boundary conditions $y(0) = 1,\ y'(0) = -1,$ $y''(0) = 1,$ and $y(1) = e^{-1},\ y'(1) = -e^{-1},\ y''(1) = e^{-1}$.

The exact solution of the equation (16) is, $y(x) = e^{-x}$

OHAM formulation described in section 2 leads to the following expression

$$L(\psi(x,p)) = \psi^{(6)}(x,p) \qquad (17)$$

$$N(\psi(x;p)) = -e^{x}\psi^{2}(x;p) \qquad (18)$$

The boundary conditions are:

$$\psi(0;p) = 1,\ \psi'(0;p) = -1,\ \psi''(0;p) = 1 \text{and}$$
$$\psi(1;p) = e^{-1},\ \psi'(1;p) = -e^{-1},\ \psi''(1;p) = e^{-1} \qquad (19)$$

Series of problems are generating by this are: zeroth order and, first order problems are defined as:

$$y_0^{(6)}(x) = \begin{cases} 0; \\ y_0(0) = 1,\ y_0'(0) = -1,\ y_0''(0) = 1, \\ y_0(1) = e^{-1}e,\ y_0'(1) = -e^{-1},\ y_0''(1) = e^{-1} \end{cases} \qquad (20)$$

$$y_1^{(6)}(x) = \begin{cases} (1+C_1)\,y_0^{(6)}(x) - e^{x}C_1 y_0^{\,2}; \\ y_1(0) = 0,\ y_1'(0) = 0, y_1''(0) = 0, \\ y_1(1) = 0, y_1'(1) = 0,\ y_1''(1) = 0 \end{cases} \qquad (21)$$

Now, to find y_0 and y_1, one can solve equations (20)-(21) and it will construct the solution for $y(x;p,C_i)$ that allows $p \to 1$ to get $y(x;C_i)$.

Zeroth-order solution: From equation (20), one can get the zeroth-order solution as:

$$y_0(x) = \frac{1}{2e}(2e - 2ex + ex^2 + 29x^3 - 11ex^3 - 46x^4 + 17ex^4 + 19x^5 - 7ex^5) \qquad (22)$$

First-order solution: By using the zeroth-order solution in equation (21) and applying the boundary conditions, one can find first-order solution as:

$$y_1(x) = \frac{C_1}{4e^2}(30240e^3x^3(108547919 - 159068768x + 62932820x^2) - 30240(-1+x)^3(177967427 + 594538266x + 1258596138x^2) + e^2(731472301108 - 26726791520578x^3 + 39170502637846x^4 + 249256847564x + 36524107238x^2 - 15497090990906x^5) + 2e(-1984084128768 + 36269284087271x^3 - 53161853727034x^4 - 676051283460x - 99054835440x^2 + 21032452715041x^5) + e^{x}(-5381734992480 + 3548102806080x - 1125876008880x^2 + 227499296640x^3 - 32590829670x^4 + 3479956572x^5 - 361x^{10} - 282482257x^6 + 17355628x^7 - 779900x^8 + 23408x^9) + e^{2+x}(-731472301108 + 3178x^9 + 482215453544x - 153003410228x^2 + 30913759200x^3 - 4428158783x^4 - 49x^{10} + 472771642x^5 - 38371719x^6 + 2357188x^7 - 105905x^8) + 2e^{1+x}(1984084128768 + 287394x^8 - 1308032845308x + 415045616364x^2 - 8625x^9 - 83862139078x^3 + 12013216410x^4 + 133x^{10} - 1282663167x^5 + 104112103x^6 - 6396130x^7)) \qquad (23)$$

Table 1: Comparison of Solutions and Absolute Error of Example 1.

x	Exact Solution	OHAM Solution (Ist Order)	Absolute Error
0.0	1.0	1.0	0.0
0.1	1.10517	1.10586	0.000686549
0.2	1.2214	1.22271	0.00130671
0.3	1.34986	1.35166	0.0018006
0.4	1.49182	1.49395	0.00212031
0.5	1.64872	1.65096	0.00223432
0.6	1.82212	1.82425	0.00213038
0.7	2.01375	2.01557	0.001817
0.8	2.22554	2.22686	0.00132328
0.9	2.4596	2.4603	0.000696879
1.0	2.71828	2.71828	0.0

Now, by adding zeroth-order and first-order solutions, and other higher order solutions if necessary, one can obtain:

$$y(x) = y_0(x) + y_1(x) + \ldots, \tag{24}$$

For the calculations of the constants C_1, using the procedure mentioned in [13-17], one can get $C_1 = 5.19711258155959 \times 10^{-13}$. By using this value of C_1, solution becomes:

$$\begin{aligned} y(x) = {} & -13758941547661921 \times 10^{-17} e^x \\ & (10653878375666761 - 2045555128673102 3x + x^2) \\ & (11037580215182167 - 19284366655837843x + x^2) \\ & (119.12894948704826 - 16.809942314320445x + x^2) \\ & (135.8305914603764 - 12.675551904732746x + x^2) \\ & (169.20738939867454 - 5.845734793308341x + x^2) \\ & -0.005145308868796304(x - 2.7199189126133523) \\ & (7.446292951546017 - 4.337782845810716x + x^2) \\ & (9.596053643993361 - 0.4778717427529698x + x^2) \end{aligned} \tag{25}$$

This is the approximate solution and comparison with the exact solution is given below in Table 2. This reveals that OHAM [13-17] yields precise results at low order of approximation. Thus one can escape from lengthy and difficult calculations

4. RESULTS AND DISCUSSIONS

OHAM formulation is presented in section 2 and test problems of formulation are presented in section 3, describing tremendously accurate solutions without spatial discretization for the problems. It is perceptible that there is certainly no need of computing further higher order terms of $y(x)$, when OHAM is used. Tables 1-2 illustrate the convergence of the absolute error $|u_{Exact} - u_{OHAM}|$ of nonlinear, homogeneous differential equations for zeroth and first order of approximations. From Tables, it is obvious that our calculations along the domain exhibit steady and consistent accuracy and specify the performance of the method for nonlinear sixth order boundary value problems. It is of worth checking that the method is perfectly approximating the solutions at less computational cost.

Table 2: Comparison of Solutions and Absolute Error of Example 2.

x	Exact Solution	OHAM Solution (Ist Order)	Absolute Error
0.0	1.0	1.0	0.0
0.1	0.904837	0.904838	6.59693×10^{-7}
0.2	0.818731	0.818734	3.65216×10^{-6}
0.3	0.740818	0.740826	8.13755×10^{-6}
0.4	0.67032	0.670332	0.0000119724
0.5	0.606531	0.606544	0.0000133398
0.6	0.548812	0.548823	0.0000116362
0.7	0.496585	0.496593	7.68683×10^{-6}
0.8	0.449329	0.449332	3.35294×10^{-6}
0.9	0.40657	0.40657	5.88617×10^{-7}
1.0	0.367879	0.367879	0.0

5. CONCLUSIONS

The intention behind this work was to explain the effectiveness and success of OHAM [13-17]. This method is simple in applicability, as it does not involve in any discretization like other numerical methods. In addition, this method gives a suitable way to manage and control the convergence by optimally determining the auxiliary constants. Moreover, OHAM converges rapidly at lower order of approximations and demonstrates its underlying potency for the solution of nonlinear problems.

REFERENCES

[1] J. Toomore, J.P Zahn, J. Latour and E.A Spiegel, "Stellar convection theory II: single-mode study of the second convection zone," A-type stars, Astrophs. J. 207, 545-563, 1976.

[2] A. Boutayeb, E. Twizell, "Numerical methods for the solution of special sixth-order boundary value problems," Int. J. Comput. Math., 45, 207-233, 1992.

[3] G. A. Glatzmaier, "Numerical simulations of stellar convection dynamics at the base of the convection zone," geophysics. Fluid Dynamics 31, 137-150, 1985.

[4] S. Chandrasekhar, "Hydrodynamics and Hydromagntic Stability," Dover, New York, 1981.

[5] P. Baldwin, "Asymptotic estimates of the eigenvalues of a sixth order boundary value problem obtained by using global phase-integral methods," Phil. Trans. Roy. Soc. London A, 322, 281-305. MR 88g: 76035, 1987.

[6] R. Agarwal, "Boundary Value Problems for Higher Order Differential Equations," World Scientific, Singapore, MR 90j:34025, 1986.

[7] M. Chawla and C. Katti, "Finite difference methods for two-point boundary value problems involving higher order differential equations," BIT, 19, 27-33. MR 80h : 65055, 1979.

[8] S. Siddiqi and E. Twizell, "Spline solutions of linear sixth order boundary value problems," Int.J. Comput. Math., 60, 295-304, 1996.

[9] A. Wazwaz, "The numerical solution of sixth order boundary value problems by the modified decomposition method," Appl. Math. Comput., 118, 311-325. MR 2001k : 65122, 2001.

[10] M. E. Gamel, J. R. Cannon and A.I. Zayed. "Sinc-Galerkin method for solving linear sixth order boundary value problems," Appl. Math. Comput. 73, 1325-1343, 2003.

[11] J.H .He, "Variational approach to the sixth order boundary value problems," App.Math.Comput. 143, 235-236, 2003.

[12] M.A. Noor and S.T Mohyud-Din, "A Reliable Approach for Solving Linear and Nonlinear Sixth-order Boundary Value Problems," Int. J. Comput. Math. ISSN 1819-4966 Volume 2, Number 2, pp. 163–172, 2007.

[12] Nicolae Herisanu, Vasile Marinca, Toma Dordea, Gheorghe Madescu, "A new analytical approach to nonlinear vibration of an electrical machine," Proceedings of the Romanian Academy, Series A 9 (3), 229–236, 2008.

[14] Vasile Marinca, Nicolae Herisanu, "Application of optimal homotopy asymptotic method for solving nonlinear equations arising in heat transfer," International Communications in Heat and Mass Transfer 35, 710–715, 2008.

[15] Vasile Marinca, Nicolae Herisanu, Constantin Bota, Bogdan Marinca, "An optimal homotopy asymptotic method applied to the steady flow of a fourth grade fluid past a porous plate," Applied Mathematics Letters 2, 245–251, 2009.

[16] Vasile Marinca, Nicolae Herisanu, Iacob Nemes, "Optimal homotopy asymptotic method with application to thin film flow," Central European Journal of Physics 6 (3), 648–653, 2008.

[17] S. Iqbal, M. Idrees, A. M. Siddiqui, A. R. Ansari, "Some solutions of the linear and nonlinear Klein–Gordon equations using the optimal homotopy asymptotic method," Appl. Math. Comput., 216, 2898-2909, 2010.

PERFORMANCE OF I-SECTIONS AS SHEAR REINFORCEMENT IN A LATERALLY LOADED SHEAR-WALL STRUCTURE.

Mahmood Memon *, Abdul Aziz Ansari **, Muhammad Rafique memon ***

ABSTRACT

Wall – Slab junction of tall building consisting of shear walls and floor slabs is one of the most highly stressed area. Possibility of junction failure increases with the increase in the height of a building. Particularly this is due to the effect of lateral forces caused by wind and earthquake. The failure is sudden, brittle and without impending warning. Therefore, attempt was made previously to increase the strength and ductility of wall – slab junction by the addition of steel wire couplets twisted together along the periphery of wall- slab junction. However, use of this type of fiber beyond 1.5% by weight is rather uneconomical and with no further appreciable improvement of the performance of junction. Shear reinforcement in the form of vertical stirrups was tried but since the slabs are thin, it is difficult to accommodate such type of reinforcement. Therefore, systematic experimental research has been carried out and based on the results details are presented about the effect of special form of reinforcement consisting of ½ inch wide "I" sections placed at various locations within the slab around the wall periphery. This type of reinforcement seems to have a very favorable effect and therefore the performance of wall – slab junction could be improved to the desired level. A method has been proposed which can be employed for the design of wall – slab junction using this reinforcement.

1. INTRODUCTION

Initially the tall buildings were designed as skeletal structure comprising of beams and columns of rolled steel sections encased in concrete and RCC floor slabs. For tall buildings it is not the gravity load but the lateral force due to wind and earthquake, which becomes the controlling factor in the analysis and design of such buildings. The effect of wind becomes more pronounced with the increase in the height of the building and it acts like a cantilever fixed at base. The skeletal structure particularly proved inadequate to provide resistance against lateral forces and therefore considerable lateral sway of these buildings caused discomfort and sense of insecurity amongst the occupants of these buildings.

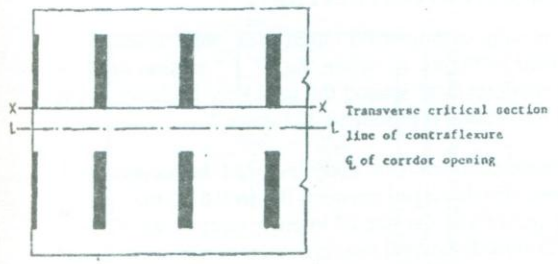

Figure 1: Plan of a typical Shear Wallbuilding showing transverse critical section

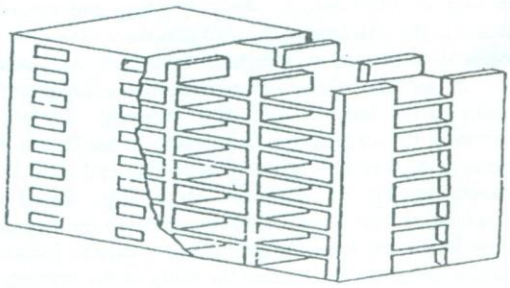

Figure 2: Perspective view of Shear Wall building showing transverse critical section

Therefore the concept of shear wall buildings consisting of load bearing cross RCC walls solely connected by floor slabs, called coupling slabs (with no beams or columns) was put forward. Typical Plan of a slab panel with pair of coupling walls is presented in Figure 1, while perspective view is presented in Figure 2.

A lot of research work has been carried out during last forty years on various aspects of the analysis and design of shear wall buildings. It was realized that full width of floor slab was not effective in resisting the lateral force because the shear induced by the lateral force was uneven with maximum intensity along the perpendicular line joining the inner faces of a pair of cross shear walls.

* Professor, department of Civil engineering, QUEST, Nawabshah, (Sindh), Pakistan, Email:bdlzz_ansari@yahoo.com
** Professor & Dean QEC, QUEST, Nawabshah, (Sindh), Pakistan, Email: dccquest@yahoo.com
*** Engineer, Gawader Sea Port, Balochistan, Pakistan.

ISSN 1665-8607

Similarly the bending moment due to lateral forces induced in the slab was maximum at the inner face of the wall and its intensity reduced drastically with the distance from this point. Therefore, the concept of effective width of slab which took part in resisting the effect of lateral forces was put forward by Qadeer & Stafford [1]. They used the numerical method of Finite Differences to evaluate the effective width of coupling slabs. Coupled shear wall with two and three bands of openings were pursued actively by Coul & Suedi [2]. Simplified analysis of coupled shear walls of variable cross-sections was presented by Pisanty & Traum [3], Coull & Wong [4] investigated the matter Design Method (DULDM) for flexural Design of common slabs where he found moment triads with the help of Elastic Finite Element analysis for the ultimate loads but found further by using Finite Element Method. Hago [5] proposed the Direct Ultimate Load design moments from these triads by applying Wood and Armer equations based on Yield Line Theory. The suitability of this method for coupling slabs was later checked by Mahmood [6]. One of the major problems is the huge concentration of shear, bending and torsional stresses in the slab around the wall periphery near its inner face. This may lead to punching failure of slab, which could be sudden, brittle, and without impending warning causing great loss of life and property. Therefore, Mahmood [6] carried out systematic research on the behaviour of wall-slab junction by testing real reinforced concrete models of relatively large size. Based on theoretical as well as experimental research he proposed the method to estimate the strength of wall-slab junction. Ghassan Elnounu [7] extended the study of the strength of wall-slab junction to other wall configurations instead of planar cross walls considered by Mahmood [6] as shown in figure. 3.

Bari [8] made use of vertical stirrups as shear reinforcement in the coupling slabs along the wall periphery to enhance its strength. Results of their findings about Stiffened Coupled Shear walls were presented by Coull et al [9]. Farrar [10] devised a method to measure

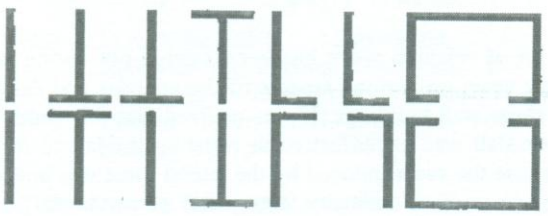

Figure 3: Different Wall Configurations

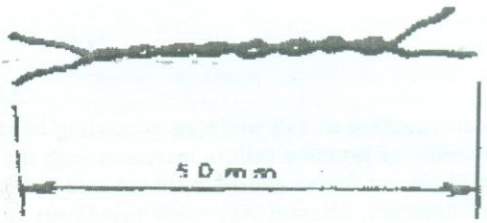

Figure 4: The sketch showing twisted twin steel fibre.

the stiffness of concerte shear walls. Johnson [11] presented his research work regarding the static and dynamic analysis of coupled shear walls. The flexural behavior of coupling slabs was investigated by Muhammad Ayoob [12]. Challal & Nollet [13] worked on upgrading the degree of coupling of coupled shear wall. Dynamic analysis of a RCC shear wall with strain rate effect was investigated by Kazushi & Akira [14]. The problem pertaining to tension flange effective width in reinforced concrete shear wall was studied by Mohammad Hassan & sheriff [15]. Since the thickness of the slab is quite commonly very small as compared with common beams, it is difficult to accommodate vertical stirrups in heavily reinforced coupling slab. Thus it was deemed imperative to provide a different type of reinforcement around wall periphery to strengthen the wall-slab connection so that punching failure could be avoided. Mahmood Memon assessed the strength of wall-slab junction under various circumstances without any shear reinforcement. Noor Ahmed [[16] made use of steel fibre consisting of twisted twins of steel wire 1 mm diameter as shown in Figure. 4. The major parameter was the ratio of fibre reinforcement, which ranged between zero to 2% by weight.

2. PRESENT INVESTIGATIONS

The testing arrangement used for this research is presented in Figure 5, while the " I " section used as shear reinforcement around the periphery is shown in Fig 6 and its location is presented in Figure 7.

The major parameters of study included the location of I-sections, which ranged between 0.5 to 0.65d, the spacing of the pieces and the rate of improvement of the ultimate load. Details of flexural reinforcement in one of the model is presented in Figure 8.

In all six models were tested. Eleven " I " section pieces used as special form of shear reinforcement at the critical section around the wall periphery at a distance of 0.5d from the sides of walls. Where d is effective depth of slab. The shear reinforcement used was 0.74 % of the critical area around the wall periphery. The cracking appeared at 40% of the ultimate load. The cracking

ISSN 1665-8607

progressed as the load increased. Several cracks appeared when the load reached 70% of ultimate load. The cracks were extended and widened when the load reached at 80% of ultimate load.

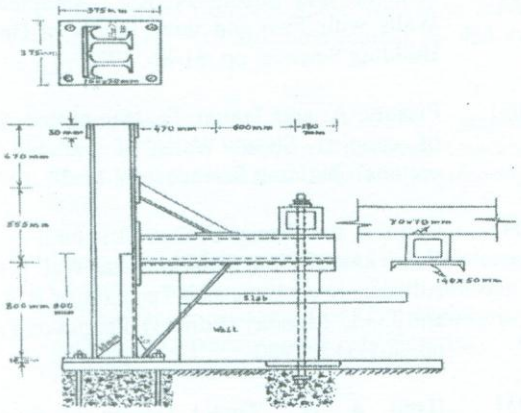

Figure 5: Dimensional details of supporting arrangement.

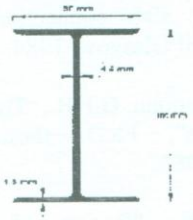

Figure 6: X-sectional view of I-section used as special form of shear

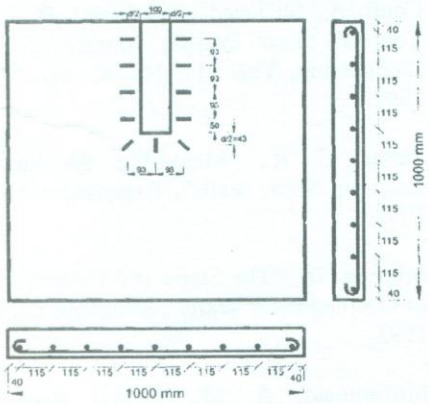

Figure 7: Arrangement of reinforcement and Location of I-sections of the model

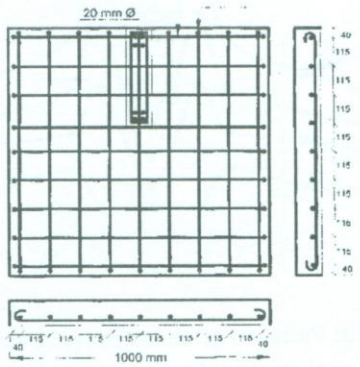

Figure 8: Arrangement of the reinforcement of the model tested

The crack pattern of this model as seen from top , bottom and the back of the model along with the measurement of distance of cracks is shown in figure 9.

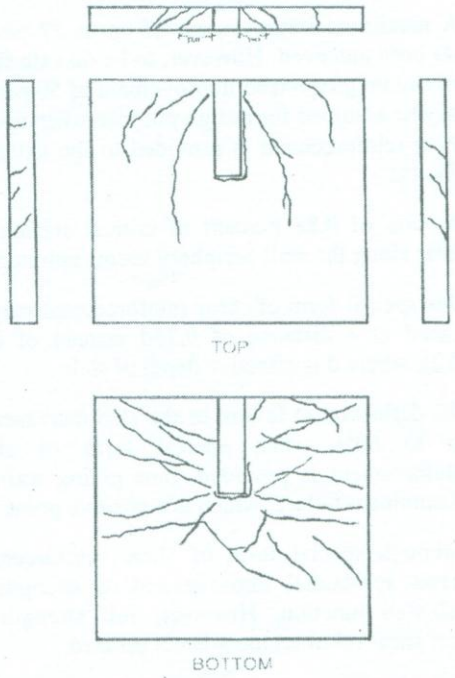

Figure 9: Crack pattern of the slab (top & bottom) with sides and back of model

Clearly this was also the shear failure due to punching of wall through the slab. The failure occurred at a load of 53.04 kN. Strain versus stress at various locations and different stages of loading are presented in figure 10.

ISSN 1665-8607

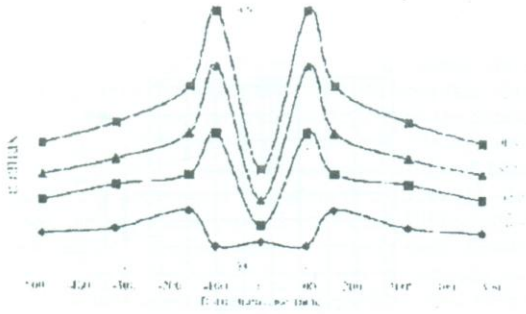

Figure 10: Variation of compressive strain in concrete along trasverse critical section different vstages of loading in the slab of SWSJWSR-02.

3. CONCLUSIONS

Based on the extensive study the following conclusion have been drawn.

01. A maximum improvement of up to 57 percent has been achieved. However, to be on safe side a maximum guaranteed improvement of 50 percent may be assumed for design purpose when special shear reinforcement is provided to the extent of 1%.

02. A ratio of 0.88 percent of critical section for shear along the wall periphery seems optimum.

03. This special form of shear reinforcement may be placed at a distance of 0.75d instead of 0.5d (d/2), where d is effective depth of slab.

04. The deflection at failure of the slab increases by up to 60% when special form of shear reinforcement is provided, thus giving warning of imminent failure, which is a positive point.

05. Although special form of shear reinforcement shows substantial improvement of strength of wall-slab junction, However, full strength of steel shear reinforcement is not utilized.

06. Amendments in the original method have been proposed to take into account the inclusion of special form of shear reinforcement revised method has been presented.

07. From the conclusions and comparison it is observed that the agreement between the actual load at failure and those predicated theoretically using proposed method is reasonable.

REFERENCES

[01] Qadeer. A. and Stafford Smith B, "The Bending Stiffness of Slab Connection Shear wall", Journal of American Concrete Institute, pp. 464-473, 1969.

[02] Coul A. and Subedi N. K., " Coupled Shear Walls with Two and three Bands of Opening", Building Science, pp. 81-86, 1972.

[03] Pisanty. A. and Traum. E., 'Simplified Analysis of coupled Shear Walls of variable Cross-sectons", building Science, pp. 11-20, 1972.

[04] Coull. A and Wong. Y. C., " Structural Behaviour of Floor slabs in Shear Wall Building, Advance in concrete slab Technology R. K. Dhir and J.G.L. Munday (Editors) Pergamon Press, pp. 301-312, 1980.

[05] Hago. A. W., "Direct Design of Reinforced Concrete Slab", Ph.D. thesis, Department of Civil Engineering, University of Glasgow, 1982.

[06] Mahmood. M.," Strength and Stiffness of shear wall Floor slab connections", Ph.D. thesis, University of Glasgow, 1984.

[07] Ghassan Elnounu. G.F.R., "Design of Shear Wall Connections", Ph.D. thesis, university of Glasgow, 1985.

[08] Bari M. S., "Design of Shear Wall-Slab Connection Using Shear Reinforcement", Ph.D. Thesis, University of Glasgow., 1987.

[09] Coull. A., Stiffened and Lamri. B., "Stiffened Coupled Shear Walls", Journal of Structural Engineering, Vol. 117, No. 8, pp. 2205-2223, 1991.

[10] Farrar. C. R., "Measuring the Stiffness of Concrete Shear walls", Experiment Mechanics, 1992.

[11] Johnson. D., "The Static and Dynamic Analysis of Coupled shear Walls", Structural Engineering. 1993.

[12] Muhammad. A. M.,"Flexural Behaviour of Reinforced Concrete coupling Slab in shear wall Structures subjected to Lateral Loads"|, M.phil thesis, mehran University, 1995.

ISSN 1665-8607

[13] Chaallal. O. and Nollet. M. J., "Upgrading the degree of Coupling of Coupled Shear walls", Journal of CSCE, 24, pp. 986-997, 1997.

[14] Kazushi. S. and Akira. W, "Dynamic Analysis of a Reinforced Concrete Shear Wall with Strain Rate Effect", ACI Structural Journal, pp. 488-49, 1998.

[15] Mohammad. H. and Sherif El-Tawil, "Tension Flang Effective Width in Reinforced Concrete Shear Walls", Journal of Structural Engineering, 2003.

[16] Noor. A. M., "Strength of steel Fibre Reinforced Concrete Shear wall-Floor Slab Junction", M.Phil Thesis, department of Civil engineering, mehran University of Engineering & Technology, jamshoro, 2003.

OPTIMIZATION OF COAL AND LIMESTONE RATIO USED IN FLUIDIZED BED COMBUSTION POWER PLANT AT LAKHRA

Shaheen Aziz*, Niaz Memon**, Suhail A. Soomro***

ABSTRACT

Due to rapidly population growth and urbanization, the power requirement is increasing every day. Thermal energy obtained from fossil fuels including coal is the prime source of power. Major part of coal reserve in Pakistan is of low-grade lignite coal containing high percentage of moisture, ash and sulphur. The low quality coal in Fluidized Bed Combustor plant at Khanote is the only power plant in Pakistan using low grade coal. Therefore its efficient utilization in proper manner is necessary in order to avoid Sulphur emissions. The effect of limestone on low grad lignite coal combustion in a fluidized bed combustor has been studied in the ratio as 5:1 to capture sulphur contents of coal. The results were compared with fluidized bed combustor in coal fired power plant at Khanote using limestone/coal ratio as 1:2. The study reveals that the limestone used in ratio of 1:5 to capture Sulphur content of coal during combustion produced almost same results when compared with ratio of 2:1 in Khanote power plant. In order to avoid various problems such as limestone preparation, bagging, transportation, handling and utilization in access, it is recommended that coal/ limestone should be 5:1 instead of 2:1.

1. INTRODUCTION

Fluidized bed combustion is the process where combustion occurr in a Fluidized bed. It is a latest technology used, especially for the utilization of low-grade coals containing high percentage of sulphur [1-2]. There are various combustors types used for the generation of electricity but research and experience shows that FBC is the best type of combustor for using low quality coals like lignite for generation of electricity. This type of combustor is environmentally safe, that's why it is also know as clean coal technology [3-4]. In the fluidized bed combustor, limestone has been used for capturing sulphur. In the bed, limestone is decomposed and reacts with sulphur dioxides in result gives calcium sulphate [5-10].

There are many advantages of fluidized bed combustion, but the main advantages are given below:

- Various low grade, high sulphur and, moisture containing coals can easily be used
- Low combustion temperature (800-950oC) can reduce the emissions of sulphur dioxide by addition of lime and can also reduce Nitrogen Oxide formation
- High heat transfer coefficient can make the required heating surface in a FBC smaller than that of a conventional boiler
- Fluidized bed combustion is environmentally safe [11-23].

The fluidization bed combustion (FBC) technology is in operation in Pakistan (3x50 MW power plant) at Khanote, Sindh, Pakistan [24-25].

Lignite type coals which are mainly used at Knaonte contain high percentage of moisture, ash and sulphur. As mentioned above, limestone in FBC reactor is decomposed and reacts with sulphur dioxide and produce calcium sulphate. FBC reactor installed at Khanote is using 2:1 coal:limestone for the treatment which can be optimized to reduce the limestone load. This study is conducted to check if stociometric ratio of sulfur presnt in caol and limestone provides similar removal efficiency. The out come of the study will help in alleviating not only operational and technical problems which occur frequently and ultimately lowers the efficiency of the power plant but also causes huge losses as a result of shut downs.

2. EXPERIMENTAL

Lakhra coal contains high percentage of moisture, ash and sulphur that is used in FBC power plant at Khanote, Sindh, Pakistan. Coal and limestone samples have been analyzed. The details of analysis are given below:

* Assistant Professor, Chemical Engineering Department, M.U.E.T, Jamshoro 76062 Pakistan
** Assistant Professor, Civil Engineering Department, QUEST, Nawabshah-67480
*** Professor, Institute of petroleum & Natural Gas Engineering, M.U.E.T, Jamshoro 76062 Pakistan

2.1 COAL ANALYSIS

(a) Proximate analysis

These types of analysis have been carried out on the compound basis. This analysis supplies readily meaningful information for coals use in stream generators. Proximate analysis determines the mass percentage of the compound i.e. moisture, volatile matter, ash and fixed carbon. Experimental work was carried out on the basis of the following methods.

(b) Moisture

About 1 gram of finally powdered air dried coal sample was weight in a crucible. The crucible was placed inside an electric hot air oven, maintained at 105-110 0C.

The crucible was allowed to remain in oven for 1 hour and then taken out with the help of pair of tongs, cooled in decicator and weighed. Then loss in weight was reported as moisture (on percentage) basis. The following formula was used as under.

%age of moisture = (loss in weight/wt:of coal taken) ×100

(c) Volatile matter

Sample was heated in the absence of oxygen in a standard test up to (954.4 0C for 7 minutes).This dried sample of coal left in the crucible was covered with a laid and placed in an electric furnace (Muffle furnace), maintained at 925+20 0C. The crucible was taken out of the over after seven minutes heating; the crucible was cooled first in air then inside a decicator and weighted again. The loss in weight calculated by the following formula.

$$\%\text{age of volatile matter} = \frac{\text{loss in wt. due to removed of volatile matter} \times 100}{\text{Wt. of coal sample taken}}$$

(d) Ash

The residual coal in the crucible obtained after volatile method was then heated without a lid in a muffle furnace at (700+50 0C) for 1/2 hour. The crucible was then taken out, cooled first in air, then in decicator and weighed. Heating, cooling and weighing is reported till a constant weight is obtained. The residue was counted as ash on the percentage basis. Thus formula was as under:

$$\%\text{age of ash} = \frac{\text{Weight of ash left} \times 100}{\text{Wt. of coal sample taken}}$$

(e) Fixed carbon

Fixed carbon was an eliminated carbon that exists in coal. In proximate analysis its determination is approximated by assuming it to be the difference between the original sample and the sum of volatile matter moisture and ash, the following formula was used as:

% age of fixed carbon = 100 - % age of (moisture + ash +volatile matter)

(e) . Ultimate analysis

The ultimate analysis of coal was carried out on the basis of element basis for precise the chemical determination. These include carbon, hydrogen, nitrogen oxygen and also sulfur. Ash was also included. The description is given as below:

(f) Carbon and Hydrogen

About 0.2 gram of accurately weighed coal sample was burnt in a current of oxygen in a combustion apparatus. Carbon and hydrogen of coal are converted into CO2 and H2O respectively. The gaseous products of combustion were absorbed respectively in KOH and CaCl2 tubes of known weights. The increase in weights of these tubes was then determined. The reactions are as follows:

Reaction:

1. $C + O_2 \rightarrow CO_2$
2. $H_2 + 1/2\ O_2 \rightarrow H_2O$
3. $2KOH + CO_2 \rightarrow K_2CO_3 + H_2O$
4. $CaCl_2 + 7H_2O \rightarrow CaCl_2.7H_2O$

The formulas for finding percentages of carbon and Hydrogen are as given below.

$$\%\text{age of C} = \frac{\text{Increase in wt. of KOH in tube} \times 12 \times 100}{\text{Wt. of coal sample taken} \times 44}$$

$$\%\text{age of H} = \frac{\text{Increase in wt. of } CaCl_2 \text{ in tube} \times 2 \times 100}{\text{Wt. of coal sample taken} \times 18}$$

(g) Nitrogen

About 1 gram of accurately weighed powdered coal was heated with concentrated sulfuric acid along with potassium sulfate K2SO4 (catalyst) in a long necked flask (called kjeldihas flask)after the solution becomes clear,it is treated with excess of KOH and liberated ammonia is distilled over and absorbed was known volume of standard acid solution. The unused acid was then determined by back titration with standard NaOH. From the volume of acid used by ammonia liberated. The percentage of nitrogen in coal have been calculated by the following formula.

$$\%\text{age of } N = \frac{\text{Volume of acid used} \times \text{normality} \times 14}{\text{Wt. of coal taken}}$$

(h) Sulphur

It is determined from the washings obtained from the taken mass sample of coal used in a bomb calorimeter for determination of calorific value. During this determination sulphur was converted into sulphates. The washings are treated with barium chloride solution. Than precipitated barium sulphate was, filtered washed and heated to constant weight. The following formula was used for the determination of Sulphur.

$$\%\text{age of S in Coal} = \frac{\text{wt.of } BaSO_4 \text{ contained} \times 32 \times 100}{233 \times \text{Wt. of coal sample taken in bomb}}$$

(i) Ash

The % age of ash determination was same as it was determined in the proximate analysis.

(j) Oxygen

The percentage of oxygen was determined by the following formula:

% age of O2 = 100 - % age of (C + H + O + N + ash)

2.2 LIMESTONE ANALYSIS

Analysis of the Limestone was carried out by using the following methods:

(a) Loss on ignition

Weigh about a 0.5-g specimen of the prepared sample to the nearest 0.001 g into a clean, previously ignited and weighed, covered platinum crucible. Heat slowly at first to avoid loss by decrepitation, finally to constant weight at 1000°C, in the muffle furnace. (Usually 1 h is sufficient for complete ignition.) Cool in a desicator and report the loss in weight as the loss on ignition.

(b) Silica oxide

Transfer the previously-ignited residue quantitatively to a 300-mL porcelain casserole. Carefully slake with about 10 mL of water, and mix to a slurry with a flat-end glass stirring rod. Add 5 to 10 mL of concentrated HC1 and digest with gentle heat until solution is complete, carefully breaking up any lumps. Evaporate to dryness and bake the residue on a sand bath or in an oven for 1 h.

If the MgO content is high (10% or over on the nonvolatile basis), bake at 120°C; if below 10% MgO, bake at 200°C. (The high dehydration temperature is efficient for low MgO, but with high MgO, silica redissolves at temperatures over 120°C). Cool to 40°C or lower, drench with concentrated HC1 and allow to stand a few minutes. Then add an equal amount of water, cover the casserole, and heat on the steam or sand bath for about 10 min. Filter through an 11-cm filter paper into a 400-mL beaker. Wash the residue thoroughly with HC1 (1:10) and then wash twice with hot (about 60-90°C) water. Pour the filtrate back into the same casserole, evaporate to dryness, treat with HC1 and water as before, filter through a second filter paper of the above type and wash twice with hot water. Save the filtrate.

Transfer the wet papers to a previously ignited and weighed platinum crucible, char carefully without allowing the paper to flame, and fmally ignite in the muffle furnace to constant weight at 1000°C (30 min is usually sufficient). Cool in a desiccator and weigh. Fuse the residue in the crucible with a little Na_2CO_3 (1 to 2 g), cool the melt, dissolve in 1:1 HC1, and add the solution to the filtrate from silica and insoluble matter.

(c) Alumina

Subtract the Fe_2O_3 from the weight of the $Fe_2O_3 + Al_2O_3$ and calculate the remainder to percentage of Al_2O_3.

(d) Iron oxide and alumina (R_2O_3)

To the acid filtrate from the silica determination, add a few drops of bromine water or concentrated HNO_3 and boil until all traces of bromine or chlorine are gone. Add enough concentrated HC1 so as to have a total volume of 10 to 15 mL of the concentrated acid. Add a few drops of methyl red solution, dilute to 200 to 250 mL, and heat to boiling. Carefully neutralize with concentrated NH_4OH until the color changes to a distinct yellow. Boil for 1 or 2 min, let settle, and filter into a 600-mL beaker. Wash four times with hot 2% NH_4C1 solution. Save the filtrate.

Place the beaker in which the precipitation was made under the funnel containing the precipitate. Dissolve the precipitate on the paper with about 15 mL of 1:1 HC1; wash the paper thoroughly with hot water. Heat, neutralize with NH_4OH, and boil as in the first precipitation. Filter (the same paper may be used) and wash four times with hot 2% NH_4C1 solution. Place the

paper in a previously ignited and weighed platinum crucible, char without allowing the paper to take fire, and fmally ignite 30 min at 1000°C in the muffle. Cool in a desiccator and weigh as R_2O_3.

(e) Calcium oxide

Combine the two filtrates from the iron oxide plus alumina determination. Make just acid to methyl red with concentrated HC1, then add 2 mL of the acid in excess. Evaporate to 350 mL, add 20 mL of 10% oxalic acid and boil. To the boiling solution add 1:3 NH4OH dropwise from a pipet until a precipitate begins to form. Now add the NH4OH still more slowly, allowing most of the precipitate to form between each addition. Continue until the methyl red just turns yellow. Add 25 mL saturated ammonium oxalate and stir. Let the solution stand and cool for 1 h.

$$\text{CaO, \%} = \frac{(\text{mL } KMnO_4) \times (\text{Normality}) \times 2.804}{\text{Weight of sample in grams}}$$

(f) Magnesium oxide

Acidify the filtrate from the calcium oxalate precipitation and evaporate to about 450 mL. Cool to room temperature. Add 30 mL of a freshly prepared 10% solution of $(NH_4)2HPO_4$. Add a few drops of methyl red, stir vigorously, and add concentrated NH_4OH slowly-especially while the precipitate is still forming—until the solution is alkaline to the methyl red. Now add 10 mL of concentrated NH_4OH for each 100 mL of solution. Stir vigorously a few times at about 15-min intervals. Let settle overnight.

Filter through a tared Gooch crucible, transferring all the precipitate to the crucible with the aid of a rubber policeman. Wash with cool 5% NH_4OH. Ignite in a muffle furnace, starting at 300°C, gradually increasing the heat to 1000°C. Hold at 1000°C for 1 h.Cool in a desiccator and weigh as $Mg_2P_2O_7$. Calculate the MgO as follows:

$$\text{MgO, \%} = \frac{\text{Weight of } Mg_2P_2O_7 \times 36.21}{\text{Weight of specimen}}$$

3. RESULTS & DISCUSSIONS

3.1 STOICHIOMETRIC REQUIREMENT OF COAL-LIMESTONE

The basis of stoicheometric calculation was taken as 100 kg of coal that contains 6% sulphur.

$$S + O_2 \rightarrow SO_2 \quad (1)$$
(32 kg) (32 kg) (64 kg)

As per equation (1), 32 kg of Sulphur reacts with 32 kg of O_2 to produces 64 kg SO_2.

Hence 6 kg of sulphur will produce = $(64/32 \times 6)$

= 12 Kg of SO_2

It means 6 Kg of sulfur produces 12 Kg of SO_2.

The SO_2 produced through reaction (1) will react with CaO and oxygen to produce $CaSO_4$ as shown in reaction (2) as follows:

$$CaO + SO_2 + 1/2O_2 \rightarrow CaSO_4 \quad (2)$$
(56 kg) (64 kg) (16 kg) (136 kg)

From reaction (2), it is clearly shown that 64 Kg of SO_2 require 56 Kg of CaO so 12 Kg of SO_2 requires:

= $(56/64) \times 12$

= 10.5 Kg of CaO

Therefore, 10.5 kg CaO is required to capture all Sulfur present in 100 Kg of Coal.

$$CaCO_3 \rightarrow CaO + CO_2 \quad (3)$$
(100 kg) (56 kg) (44 kg)

56 kg of CaO produced from 100 kg of $CaCO_3$.

10.5 kg of CaO produce 18.75 kg (100/56 x 10.5)

Therefore, CaCO3 = 18.75 kg

Lime Stone having 95% $CaCO_3$

95 kg. $CaCO_3$ - - - - - - - - 100 kg Of lime Stone

Therefore

18.75 kg. $CaCO_3$ - - - - - 100/95 x 18.75 = 19.74 kg of lime Stone.

Therefore, for 100 kg coal having 6 kg (6%) sulphur will require 19.74 kg.

Lime Stone having 95% $CaCO_3$.

Therefore Coal-lime stone ratio is 100:20 or 5:1.

In table-1, the result clearly shows 6% of sulphur present in coal. The limestone is being used to capture the Sulphur (6%) present in the coal. Practically, in the power plant, coal-limestone ratio of 2:1 is being used. But as per stoichiometric requirement that has been shown above as per above calculation it shows that coal-limestone ratio should be 5:1 that is required for capturing of sulphur (6%) present in coal. Figure. 1 gives the comparison between amounts of limestone required actually with that required stoichi metirically.

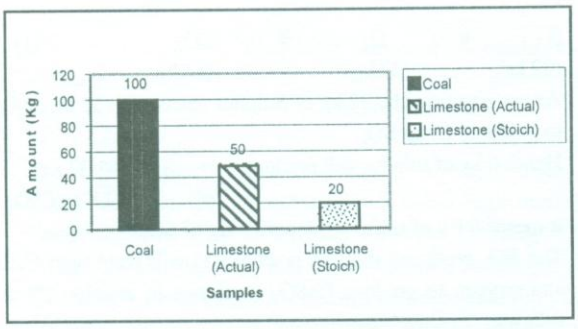

Figure 1: Comparison of Limestone Usage with Actual and Stoichiometrical Calculations

3.2 OTHER FACTORS AFFECTING THE EFFICIENCY OF FBC

As per specification of the FBC, coal & limestone must go through a process of crushing & grinding in order to get the proper size of the material to be burnt in the FBC. As it was noticed that, there is 150% excess limestone used that is to be crushed, it not only causes energy loss but also extra financial burden on the FBC plant.

Excess of limestone create various problems in the FBC that includes the formation of bottom ash & fly ash that ultimately causes maintenance, handling & disposal problems.

Due to the improper ratio of limestone supply, the generation tubes and wings/ blade of I.D fans were eroded. Filter bags were also ruptured and resulting in frequent shut down of power generation units.

4. CONCLUSIONS

As per stoichiometric requirement 5:1, coal / limestone ratio is required, but practically in FBC in the power plant 2:1 is being used. This shows150% excess quantity of limestone is being used. Huge amount is being wasted for 150% excess quantity of limestone. The excess amount of limestone not only causes loss of money but also causes various problems including damage of FBC internal chamber walls, ID Fans that affect the efficiency of power plant.

RECOMMENDATIONS

- The ratio of coal and limestone should be used on the basis of Sulphur contents.
- Due to higher percentage of particles in the flue gases the blades/wings of I.D fans are being eroded.
- Regular analysis of the following should be done for the determination of Sulphur compounds and calcium oxide.
  - Coal particle size at feed point
  - Limestone particle size at feed point
  - Fly ash composition
  - Bottom ash composition
  - Re-injection (un-burnt material) composition
  - Flue gases composition

REFERENCES

[1] Douglas, M, "Energy Technology", Hand Book, Conceding Edition, Mc Graw Hill, New York, 1977.

[2] Lopez, S. B, Bohm, V. N, "Public policy for energy technology innovation - A historical analysis of fluidized bed combustion development in the USA", J. Energy Policy, no. 30, 1173 –1180, 2002.

[3] The Coal Industry Advisory Board, "The Use of Coal in Industry", International Energy Agency, OECD, Paris, 1982.

[4] Yang, W.C, Handbook of fluidization & fluid particle systems (chemical industries), 2007.

[5] Begic, F, Afgan,N. H, "Sustainability assessment tool for the decision making in selection of energy system - Bosnian case", available on line on www.sciencedirect.com , J Energy, 2007.

[6] Nam, C. H, Pfeffer, R, "Aerated vibro-fluidization of silica nano-particles", published online, Wiley inter science, vol. 50, no.8, August 2004.

[7] Go´ra, D., Anthony, E.J., Bulewicz, E.M., 'Steam reactivation of 16 bed and fly ashes from industrial-scale coal-fired fluidized bed combustors", J Fuel, 85, 94–106, 2004.

[8] Ferrer, E., Aho, M., Silvennoinen, J., Nurminen, R., "Fluidized bed combustion of refuse-derived fuel in presence of protective coal ash", J. Fuel Processing Technology 87, 33 – 44, 2005.

ISSN 1665-8607

[9] Knapp. R, "Clean Coal use- a Reliable Option Sustainable Energy Developments", Workshop organized by the Central Mining institute and UNECE in Szczyrk, Poland-24-26, May 2001.

[10] Knapp. R, "Energy and Environment in the 21st century- challenges and cooperation in the Asia pacific region", (session B3 Environment, B3 clean coal Technology) held in Toyo- 18-19 October 2000.

[11] Changdu and Sichvan, " 3x50 MW FBC Lakhra power plant Near Khanote", Dong Fang Electric corporation, R. of China, 1993.

[12] Changdu and Sichvan, "The structure, operation and Maintenance of 220 t/hr Fluidized Boiler", Dong Fang Electric corporation, Book-I, Rep. of China, 1992.

[13] Water and Power Development Authority, Brochure, "150 MW Lakhra Power station Near Khanote", 1993.

[14] Martin. C, Villamanan, M. A, Chamorro, C. R, Otero. J, Cabanillas. A, Segovia J. J., "Low-grade coal and biomass co-combustion on fluidized bed: energy analysis", J. Energy 31, 330–344, 2006.

[15] Takuwa. T, Naruse. I, "Emission control of sodium compounds and their formation mechanisms during coal combustion", Proceedings of the Combustion Institute 31, 2863 –2870, 2007.

[16] Manovic. V, Grubor, B., Loncarevic, D., "Modeling of inherent SO2 capture in coal particles during combustion in Fluidized bed", J Chemical Engineering Science 61 ,1676 –1685, 2006.

[17] Ishom,F., Harada, T., Aoyagi, T., Sakanishi, K., Korai, Y., Mochida, Isao., "Problems in PFBC boiler (2): characterization of bed materials found in a commercial PFBC boiler at different load levels", J. Fuel 83, 1019–1029, 2004.

[18] Flemming.F "Deposit formation and corrosion in the air preheater of a straw fired combined Heat and power production Boiler", IFRF journal in May-2002.

[19] Aziz .S, Pathan., M.I., Soomro, S.A, "Erosion Problems in FBC Power Plant Based On Lakhra Coal", J.Appl. & Emerg. Sc., Vol. 1, No.03, P-145, 2006.

[20] Valentim, B., Lemos de Sousa, M.J., Abelha., P., Boavida,D., Gulyurtlu, I., "The identification of unusual microscopic features in coal and their derived chars: Influence on coal fluidized bed combustion", International Journal of Coal Geology 67, 202- 211, 2006.

[21] Zhou, H., Flamant, G., Gauthier, D.,, "DEM-LES simulation of coal combustion in a bubbling fluidized bed Part II: coal combustion at the particle level", Chemical Engineering Science 59, 4205 –4215, 2004.

[22] Zhou, H., Flamant, G., Gauthier, D., "DEM-LES of coal combustion in a bubbling fluidized bed. Part I: gas-particle turbulent flow structure", Chemical Engineering Science 59, 4193 –4203, 2004.

[23] Dennis J.S, Hayhurst, A.N., Scott, S.A., "The combustion of large particles of char in bubbling fluidized beds: The dependence of Sherwood number and the rate of burning on particle diameter", J. Combustion and Flame, 147, 185–194, 2006.

[24] Raffle, M., Willert, C.E, Wereley, S. T, Kompenhans, J, "Particle image velocinmetry: A practical guide (experimental fluid mechanics)", 2nd revised edition, June 2007.

[25] Aziz .S, "study of technical aspects for improving the efficiency of FBC power plant at Khanot" M.E Thesis, Chemical Engineering Department, Mehran University of Engineering & Technology, Jamshoro, 1999.D. Broadbent, "Reactive dyes," in *Basic principles of textile coloration*, A. D. Broadbent, Ed., First ed: Society of Dyers and Colourists, pp. 332-357, 2005.

ISSN 1665-8607

Table 1: Proximate Analysis of Coal

S.#	Calorific Value (Kcal/kg)	Sulphur	Moisture (% age)	Ash (% age)	Volatile Matter (% age)	Fixed Carbon (% age)
1.	3336	06.73	16.90	30.05	26.03	21.51
2.	3297	06.23	16.94	30.23	27.15	21.93
3.	3315	05.78	16.45	31.84	25.54	20.34
4.	3225	06.12	16.33	30.34	26.91	21.93
5.	3296	05.96	16.51	30.41	26.92	21.73
6.	3190	05.86	16.30	30.91	25.32	21.45
7.	3217	06.12	16.20	30.74	26.01	20.31
8.	3189	06.23	16.09	31.38	25.40	20.39
9.	3219	06.25	16.31	30.29	26.50	21.13
10.	3326	05.92	16.57	31.91	25.03	21.20
11.	3251	05.78	16.14	30.01	26.21	20.20
12.	3295	06.69	16.31	30.12	26.59	21.50
13.	3293	06.15	16.14	30.13	26.89	21.50
14.	3253	06.31	16.75	31.03	26.30	20.90
15.	3292	06.21	16.39	30.05	26.89	20.30
Average	3266	06.15	16.42	30.62	26.41	21.02

Table 2: Ultimate Analysis of Coal

S.#	Moisture (% age)	Ash (% age)	Sulphur (% age)	Carbon (% age)	Hydrogen (% age)	Nitrogen (% age)	Oxygen (% age)
1.	08.49	30.00	05.39	38.99	07.54	00.70	08.890
2.	32.00	19.52	05.20	33.04	02.45	00.75	07.040
3.	30.76	12.44	05.32	40.31	03.09	00.76	07.510
4.	32.46	06.49	03.32	45.70	03.48	00.92	07.630
5.	29.86	06.50	04.31	47.17	03.61	00.89	07.660
6.	30.65	10.14	05.23	42.10	03.35	00.73	07.350
7.	29.75	11.15	04.25	41.81	03.34	00.39	07.890
8.	30.45	10.75	04.23	41.91	03.93	00.65	07.130
9.	29.35	10.85	04.92	42.21	03.45	00.78	07.390
10.	30.25	09.35	04.31	40.20	03.41	00.97	07.210
Average	28.40	12.71	05.07	41.34	04.11	00.75	07.57

Table 3: Analysis of Limestone

S. #	LOI (% age)	SiO_2 (% age)	Al_2O_3 (% age)	Fe_2O_3 (% age)	CaO (% age)	MgO (% age)	SO_3 (% age)
1.	37.49	09.52	00.56	00.48	50.49	00.80	00.17
2.	36.23	08.92	00.52	00.47	51.23	00.70	00.18
3.	38.75	10.12	00.61	00.49	49.75	00.90	00.16
4.	37.51	09.62	00.49	00.39	52.01	00.80	00.19
5.	37.47	09.42	00.63	00.57	48.97	00.60	00.15
6.	36.92	09.34	00.59	00.50	51.60	00.90	00.14
7.	38.06	09.70	00.53	00.46	49.38	00.80	00.20
8.	37.23	09.54	00.63	00.50	51.01	00.70	00.17
9.	37.75	09.50	00.49	00.47	49.97	00.80	00.17
10.	37.43	09.51	00.55	00.45	50.48	00.80	00.18
Average	37.484	9.519	0.56	0.478	50.489	0.78	0.171

KNOWLEDGE MANAGEMENT AWARENESS AND USAGE IN BANKING SECTOR OF PAKISTAN

Shabina Shaikh*, Abdul Sattar Jamali**

ABSTRACT

This research paper aims to measure the knowledge management awareness and knowledge management usage in banking sector of Pakistan. For this study public and private banks, NBP (National Bank of Pakistan) and UBL (United Bank Limited), are selected from Pakistani banking sector. Comparative study is done after evaluating knowledge management awareness and usage. Questionnaire is used to gather quantitative data from managers of both banks. 35 managers from 15 branches of each bank are selected for gathering data. The result visibly shows the level of knowledge management awareness and its usage in both NBP (National Bank of Pakistan) and UBL (United Bank Limited). Moreover, result also proved KM awareness in employees of public banks is lesser than employees of private banks and KM usage in employees of private banks is higher than employees of public banks.

1. INTRODUCTION

The knowledge management is the concept in which organisations intentionally collect, organise, share and analyse their knowledge within the resources, documents and qualifications of employees [1]. Managing and leveraging knowledge thus has to be at the core of any attempt to improve an organisation's performance [2].

Knowledge management in the business sector started in the early 1990's when organisations realised KM, it is essential to every organisation and can give the organisation a competitive advantage if the knowledge assets are utilised more effectively and wisely [3]. According to Angus & Patel [4], an article published in Information Week, the knowledge management is the name of a concept in which an enterprise consciously and comprehensively gathers, organises, shares, and analyses its knowledge in terms of resources, documents, and people skills. Knowledge management ensures that "knowledge" is used as effectively and efficiently in achieving organisational goals. As a result, the knowledge management becomes essential factor in the creation and management of intangible asset of an organisation.

The modern business world is characterized by dynamic and changing markets and continuous technological advance [5]. To deal with these trends, organizations must become more flexible and one certain way for them to do so is to strengthen their potential to learn as organizations. Thus, "knowledge" becomes an essential organizational driver and a key factor in value creation.

In today's banking sector where knowledge management is the essential part of growth is been neglected. We need to be able to understand knowledge management better, and to find ways to measure it and identify best practices in this area so that banks can operate better and can develop policies to help them to do so.

The purposes of this study are:

1. Promoting innovation
2. Enhancing the skill level of employee with the help of knowledge management awareness,
3. Endorsing the importance of knowledge management practices for leveraging performance,
4. Recognising the impact of organisational culture on knowledge management.

The study has two research questions:

1. Does Pakistani banking sector, including public and private banks, have knowledge management awareness?
2. Does Pakistani banking sector use knowledge management strategies?

The objectives of this study are:

1. Measuring the level of knowledge management awareness in Pakistani banks in public and private banks.
2. Evaluating the level of knowledge management usage in Pakistani banks in public and private banks

* Department of Management Sciences, Isra University, Hyderabad, Pakistan, Email: shabinashaikh@gmail.com
** Department of Mechanical Engineering, QUEST, N/SHAH.

Hypotheses of this study are:

1. KM awareness in employees of public banks will be lesser than employees of private banks.
   Statistically H1 can be represented as: KM $\text{Awareness}_{NBP} < \text{KM Awareness}_{UBL}$
2. KM usage in employees of private banks will be higher than employees of public banks.
   Statistically H2 can be represented as: KM $\text{Usage}_{UBL} > \text{KM Usage}_{NBP}$

2. LITERATURE REVIEW

Davenport and Prusak [6] give an extensive definition of knowledge: "Knowledge is a fluid mix of framed experience, values, contextual information, and expert insight that provides a framework for evaluating and incorporating new experiences and information. It originates and is applied in the minds of knower".

There is no single agreed definition of knowledge presently and there remain many competing theories. Knowledge involves complex cognitive processes: perception, learning, communication, association and reasoning. The term knowledge is also used to mean the understanding of a subject with the ability to use it. Davenport and Prusak [7] explain that knowledge exists within people. Knowledge derives from information as information derives from data. The authors conceive that if information is to become knowledge, humans must do virtually all the work.

The term knowledge is defined in the Oxford Dictionary and Thesaurus [8] as: "awareness or familiarity gained by experience (of a person, fact, or thing)", "specific information; facts or intelligence about something", or "a theoretical or practical understanding of a subject".

We often divide knowledge into two types, tacit and explicit knowledge [9]. By tacit knowledge we mean knowledge that a human is unable to express, but is guiding the behavior of the human. Explicit knowledge is knowledge that we can represent, or "codify", for example in reports, books, talks, or other communication.

Knowledge Management comprises a range of practices used by organizations to identify, create, represent, and distribute knowledge [10]. Knowledge Management programs are typically tied to organizational objectives such as improved performance, competitive advantage, innovation, developmental processes, lessons learnt transfer (for example between projects) and the general development of collaborative practices. Knowledge Management is frequently linked and related to what has become known as the learning organization, lifelong learning and continuous improvement

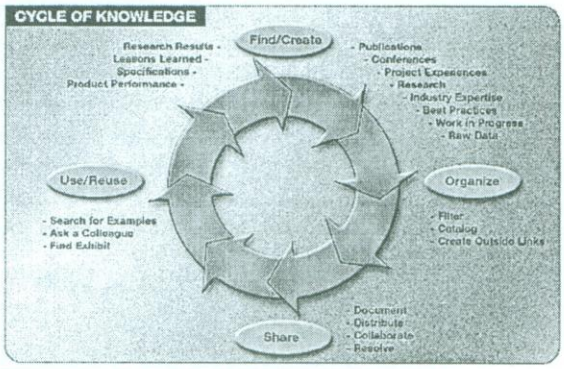

Figure 1: Knowledge Management Cycle [11]

In traditional organizations, knowledge leans to flow along organizational lines, from the top to bottom. But that prototype rarely gives outcomes in making knowledge available and where it's needed the most. In contemporary organizations, information can flow transversely organizational lines, reaching knowledge holders who can use it in ways that best endorse the organizational goals and that improves responsiveness to the customer at the same time. By investigating the four basic elements of the knowledge management cycle, we can understand it better [Figure 1] (Mike Burk) [11]: find/create, organize, share, and use/reuse. Under "find/create," especially as it functions in a transportation organization, knowledge can be gathered through a many ways, including seminars, publications, conferences, workshops, meetings, project experiences, research, and organizational skills. After that in the cycle, "organize," the knowledge is scanned and is linked with the outside sources. Then the information is shared for broad accessibility, making utilize of databases, internet and other techniques.

To help carry out the "organize" and "share" works in knowledge domains of knowledge holders having a familiar interest, many experts recommend a knowledge manager. This person has the task of soliciting good practices, indexing and cataloguing new information as it comes in, and serving as an information broker by assisting people to obtain the information they need. The

knowledge manager can also serve as a supporter for knowledge transfer and sharing practices within and further than his knowledge domain of work.

The final stage of the knowledge management cycle, "use/reuse," occupies both informal contacts and access to reports, good practices, success stories, and other forms of communication, including exhibits, demonstrations, and training sessions. To a great extent of this knowledge can be made accessible to an extensive audience through the Internet. This is the step in which knowledge is functional to solve real-world issues, working more efficiently, and improving safety. Of course, these results are then saved as part of the lessons learnt for use as the knowledge cycle starts again.

3. RESEARCH METHODOLOGY

For measuring the level of knowledge management awareness 10 questions are asked from employees, questions carry measures which focus on knowledge management awareness (Table 1)

Table I: Measures related to KM awareness

Questions	Measures
Q.1	KM under different name
Q.2	Responsibility of manager
Q.3	Information overloaded
Q.4	Understanding of KM
Q.5	Number of clients
Q.6	Improve worker efficiency
Q.7	Knowledge sharing vertically
Q.8	Responsibility of the knowledge officer
Q.9	Knowledge sharing horizontally
Q.10	New knowledge creation

For measuring the level of knowledge management usage 10 questions are asked, questions carry measures which focus on knowledge management usage (Table 2)

Table 2: Measures related to KM usage

Questions	Measures
Q.1	Value System
Q.2	Capturing knowledge from other sources
Q.3	Formal training related to KM
Q.4	Responsibility of KM unit
Q.5	knowledge worker retention
Q.6	Grant resources to obtain external knowledge
Q.7	Informal training related to KM
Q.8	Transfer of knowledge
Q.9	Knowledge management strategy
Q.10	Database of lessons learned

SPSS (Statistical Package for the Social Sciences) 16.0 is used for descriptive and inferential statistics. Statistics are a method of summarizing and analyzing data for the purpose of drawing conclusions about the data. Descriptive statistics simply offer us a way to describe a summary of data. Whereas inferential statistics allow us to make a conclusion related to hypothesis.

The sample size has a direct impact on the power of statistical analysis and the generalizability of results (Hair et al., 1998). The study is aims to measure the level knowledge management awareness and usage which is done through the survey of two banks that is National Bank of Pakistan (NBP) and United Bank Limited (UBL). Nine branches of each bank are selected on random basis by questioning of 35 managers from each bank; selection of managers is also done through random basis.

4. ANALYSIS OF RESEARCH

(a) Knowledge management awareness in National Bank of Pakistan (NBP)

Table 3 presents measures related to questions along with their mean values related to KM awareness. Average mean measures the level of KM awareness.

Table 3: Measures related to KM awareness along with mean values of NBP

Questions	Measures	Mean
Q.1	KM under different name	3.06
Q.2	Responsibility of manager	3.00
Q.3	Information overloaded	3.37
Q.4	Understanding KM	3.20
Q.5	Number of clients	3.14
Q.6	Improve worker efficiency	3.03
Q.7	Knowledge sharing vertically	2.91
Q.8	Responsibility of the knowledge officer	2.06
Q.9	Knowledge sharing horizontally	3.00
Q.10	New knowledge creation	2.94
	Grand Mean	2.97

The scale of measurement is from 0 – 4, 0 represents strongly disagree and 4 represents strongly agree to the question. The mean value of question 1 from the employees of NBP is 3.06 which means most of employees agreed that in their organization KM is practicing but with different name. For question 2 most of employees agreed KM is the responsibility of managers which we came to know from the mean value

3.00. The mean value 3.37 of question 3 says that information is basically overloaded in their bank. Most of employees of NBP agreed that they do have much understanding about KM which is calculated from the mean value 3.20 of question 4. NBP's employee do believe that implementing KM in their bank will increase number of clients and can improve workers' efficiency as well, which we come to know from the mean values 3.14 and 3.03 of questions 5 and 6 . Employees of NBP also believe that implementing KM can increase knowledge sharing horizontally which says by the mean value 3.00 of question 9. For question 7, 8 and 10 mean values are in between 2-3, it means employees are not sure whether implementing KM in banks increase knowledge sharing vertically or not, also they are not aware of knowledge officer's responsibility and they don't know if top management takes keen interest in creation of new knowledge or not.

With the help of mean values (Figure 2), average mean is taken out which is 2.94. Average mean gives us the percentage value which is 74.25. If we rank KM awareness in NBP out of 100, 74.25 is the result we get.

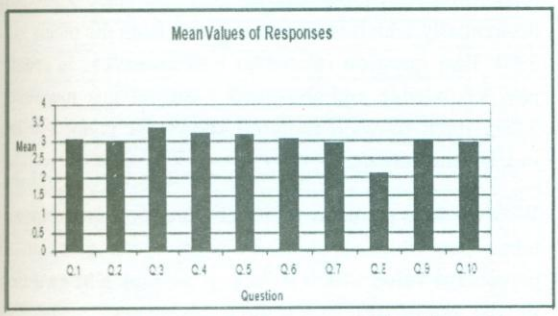

Figure. 2: Mean Values of Responses Related to KM Awareness in NBP

Result shows KM awareness 74 percent in NBP and rest 26 percent is unawareness about KM in NBP (Figure 3).

The rest 26 percent shows where lacking is, where NBP needs to know about KM.

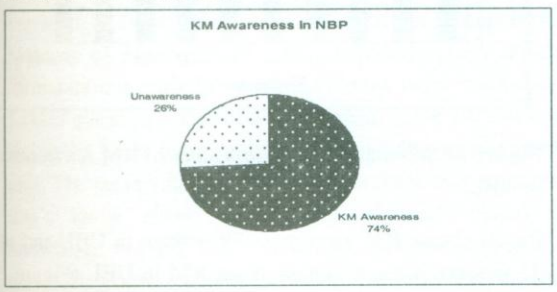

Figure. 3: KM Awareness in NBP

(b) Knowledge management Usage in National Bank of Pakistan (NBP)

Table 4 presents measures related to questions along with their mean values related to KM usage. Average mean measures the level of KM usage.

Table 4: Measures related to KM usage along with mean values of NBP

Questions	Measures	Mean
Q.1	Value System	1.23
Q.2	Capturing knowledge from other sources	3.00
Q.3	Formal training related to KM	3.00
Q.4	Responsibility of KM unit	1.03
Q.5	knowledge worker retention	1.03
Q.6	Grant resources to obtain external knowledge	2.97
Q.7	Informal training related to KM	1.14
Q.8	Transfer of knowledge	1.03
Q.9	Knowledge management strategy	1.06
Q.10	Database of lessons learned	2.80
	Grand Mean	1.82

The scale of measurement is from 0 – 4, 0 represents strongly disagree and 4 represents strongly agree to the question. Mean value 1.23 of question 1 shows mostly employees of NBP disagreed about the value system related to KM in their organization. As per the mean value of question 2, which is 3.00, says NBP captures knowledge from other sources such as competitors. Majority of employees of NBP agreed that they do get formal trainings which we come to know from mean value 3.00 of question 3. Question 4, 5 and 8 got same mean value which is 1.03; it shows mostly in NBP there isn't any knowledge management unit, employees don't know about the policies planned related to knowledge workers and there isn't any separate function of knowledge transfer. Mean value 2.96 of question 6 shows that NBP grants resources to obtain external knowledge. As per the mean value of question 7 which is 1.14 shows that there isn't any informal training provided to NBP employees. Mean value of question 9 is 1.06 which clearly shows that NBP doesn't have any written knowledge management policy. For updating database of lessons learned, employees' responses gave mean value 2.8 which reflects that employees do update database.

With the help of mean values (Figure 4), average mean is taken out which is 1.82. Average mean gives us the percentage value which is 45.7. If we level KM usage in NBP out of 100, 45.7 is the result we get.

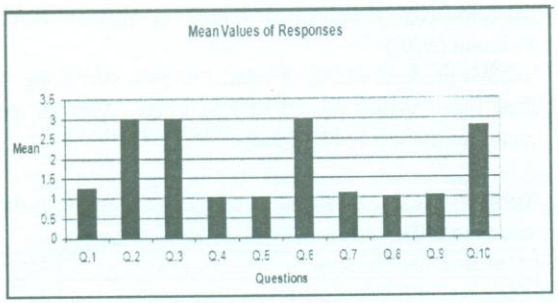

Figure. 4: Mean Values of Responses Related to KM Usage in NBP

Result shows KM usage 46 percent in NBP and rest 54 percent is gap which makes KM unsuccessful in NBP (Figure 5). The rest 54 percent shows where lacking is, where NBP needs to use more KM strategies.

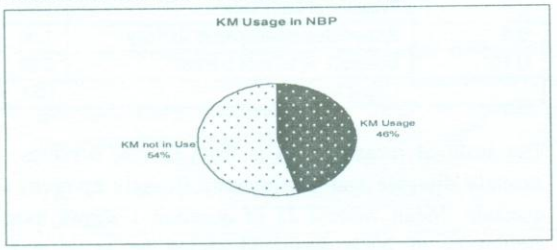

Figure. 5: KM Usage in NBP

(c) Knowledge management awareness in United Bank Limited (UBL)

Table 5 presents measures related to questions along with their mean values related to KM awareness. Average mean measures the level of KM awareness.

Table 5: Measures related to KM awareness along with mean values of UBL

Questions	Measures	Mean
Q.1	KM under different name	3.17
Q.2	Responsibility of manager	3.26
Q.3	Information overloaded	3.40
Q.4	Understanding KM	3.14
Q.5	Number of clients	3.11
Q.6	Improve worker efficiency	3.29
Q.7	Knowledge sharing vertically	3.00
Q.8	Responsibility of the knowledge officer	2.91
Q.9	Knowledge sharing horizontally	3.06
Q.10	New knowledge creation	3.20
	Grand Mean	3.15

The scale of measurement is from 0 – 4, 0 represents strongly disagree and 4 represents strongly agree to the question. The mean value of question 1 from the employees of UBL is 3.17 which means most of employees agreed that in their organization KM is practicing but with different name. For question 2, the mean value is 3.26, most of employees agreed KM is the responsibility of managers. The mean value of question 3 which is 3.4 says that information is basically overloaded in their bank. Most of employees also agreed that they do not have much understanding about KM because mean value of question 4 is 3.15. They do believe that implementing KM in their bank will increase number of clients which we come to know from mean value of 3.00 of question 5 and can improve workers' efficiency as well which we come to know from mean value 3.00 of question 6. With the mean value of 3.00 of question 7 we come to know employees of UBL also believe that implementing KM can increase knowledge sharing horizontally. Mean value of question 8 is 2.91, which shows employees are not aware of knowledge officer's responsibility. Employees of UBL do share knowledge horizontally which we come to know from the mean value 3.06. Last question related to KM awareness is creating new knowledge and the mean value of this measure is 3.20, which shows if required knowledge is not available in UBL they create it.

With the help of mean values (Figure 6), average mean is taken out which is 3.15. Average mean gives us the percentage value which is 78.8. If we rank KM awareness in UBL out of 100, 78.8 is the result we get.

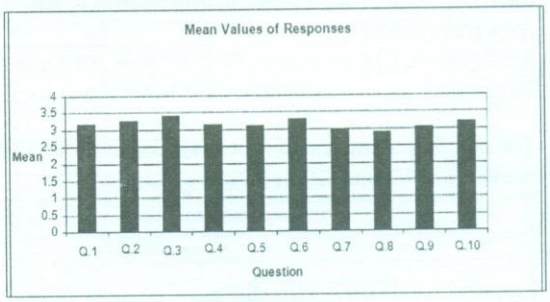

Figure 6: Summary of Mean Values of KM Awareness in UBL.

Result shows KM awareness 79 percent in UBL and rest 21 percent is unawareness about KM in UBL (Figure 7). The rest 21 percent shows where lacking is, where UBL needs to know more about KM.

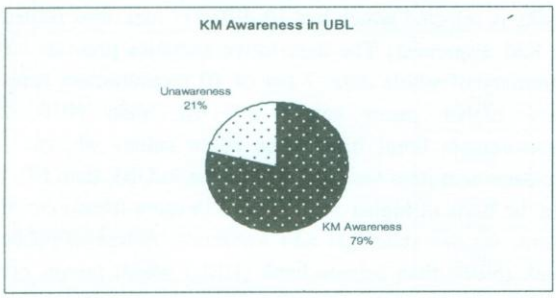

Figure. 7: KM awareness in UBL

(d) Knowledge management awareness in United Bank Limited (UBL):

Table 6 presents measures related to questions along with their mean values related to KM usage. Average mean measures the level of KM usage.

Table 6: Measures related to KM usage along with mean values of UBL

Questions	Measures	Mean
Q.1	Value System	1.31
Q.2	Capturing knowledge from other sources	3.00
Q.3	Formal training related to KM	3.00
Q.4	Responsibility of KM unit	1.03
Q.5	knowledge worker retention	2.63
Q.6	Grant resources to obtain external knowledge	3.03
Q.7	Informal training related to KM	1.11
Q.8	Transfer of knowledge	1.09
Q.9	Knowledge management strategy	1.91
Q.10	Database of lessons learned	3.31
	Grand Mean	2.14

The scale of measurement is from 0 – 4, 0 represents strongly disagree and 4 represents strongly agree to the question. Mean value 1.31 of question 1 shows mostly employees of UBL disagreed about the value system related to KM in their organization. As per the mean value of question 2, which is 3.00, says UBL captures knowledge from other sources such as competitors. Majority of employees of UBL agreed that they do get formal trainings which we come to know from mean value 3.00 of question 3. Question 4 got mean value 1.03 which shows in UBL there isn't any knowledge management unit. The mean value 2.63 of question 5 shows employees don't know about the policies planned related to knowledge workers. Mean value 3.03 of question 6 shows that UBL grants resources to obtain external knowledge. As per the mean value of question 7 which is 1.11 shows that there isn't any informal training provided to UBL employees. Mean value of question 9 is 1.91 which clearly shows that UBL doesn't have written knowledge management policy. For updating database of lessons learned, employees' responses gave mean value 3.31 which reflects that employees do update database.

With the help of mean values (Figure 8), average mean is taken out which is 2.14. Average mean gives us the percentage value which is 53.3. If we level KM usage in NBP out of 100, 53.3 is the result we get.

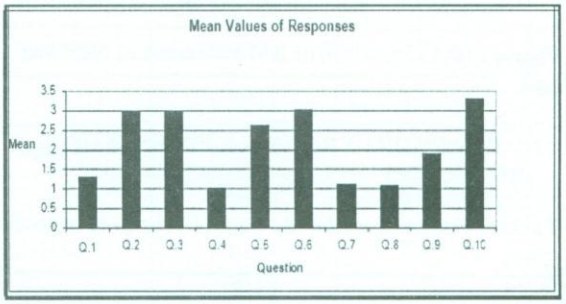

Figure 8: Mean Values of KM usage in UBL

Result shows KM usage 53 percent in UBL and rest 47 percent is gap which makes KM unsuccessful in UBL (Figure 9). The rest 47 percent shows where lacking is, where UBL needs to use more KM strategies.

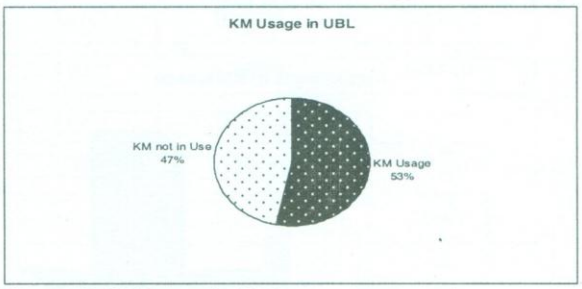

Figure 9: KM usage in UBL

4.1 COMPARISON OF KM AWARENESS FINDINGS OF BOTH CASES

Table 7: Percentages of KM Awareness Findings of Both Cases

NBP	UBL
74.2%	7.8%

Figure 10 presents the comparison of KM awareness in NBP and UBL through the percentage values they carry. NBP is on 74% whereas UBL is on 78%. It clearly shows

that UBL is ahead than NBP in KM awareness.

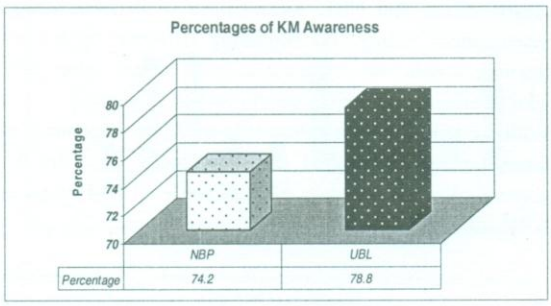

Figure . 10: Comparison of KM awareness of NBP and UBL

4.2 COMPARISON OF KM USAGE FINDINGS OF BOTH CASES

Table 8: Percentages of KM Usages Findings of Both Cases

NBP	UBL
45.7%	53.3%

Figure 11 presents the comparison of KM usage in NBP and UBL through the percentage values they carry. NBP is on 45% whereas UBL is on 53%. It clearly shows that UBL is ahead than NBP in KM usage.

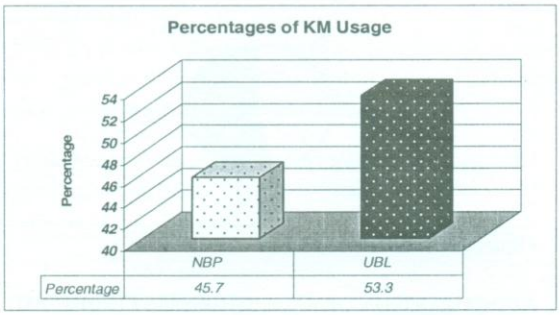

Figure. 11: Comparison of KM usage of NBP and UBL

4.3 HYPOTHESES TESTING

Hypothesis 1 (H1) is, KM awareness in employees of public bank will be lesser than employees of private bank. Statistically can be represented as: $KM\ Awareness_{NBP} < KM\ Awareness_{UBL}$

Table 9 presents the descriptive statistics of hypothesis 1. For hypothesis 1 the variable KM awareness of both banks is selected which has 10 different measures related to KM awareness. The descriptive statistics presents the summary of whole data. 7 out of 10 measurement items have higher mean values in UBL than NBP, 2 measurement items have same mean values whereas 1 measurement item has less mean value in UBL than NBP. On the basis of higher mean values in more measurement items, we can state that KM awareness is less in public bank (NBP) than private bank (UBL) which proves our hypothesis 1 valid.

Table 10 shows the T test (Statistical formula of T-test is t = [(x1 - x2) - d] / SE) of hypothesis 1, which is used to test whether there is a significant differences between the means of two groups. Since we are using a 95% confidence, alpha = 0.05, therefore if $p < 0.05$ we accept our hypothesis and reject null hypothesis. Under the "t-test for Equality of Variances" the "Sig." for "Equal variances assumed", 6 out of 10 measurement items have less than 0.05 values, therefore we can say there is a significant difference between the variance of two groups.

Table 9: Descriptive statistics of hypothesis 1

Group Statistics

	ID	N	Mean	Std. Deviation	Std. Error Mean
KM under different name	NBP	35	4.0571	0.23550	0.03981
	UBL	35	4.1714	0.38239	0.06463
Responsibility of managers	NBP	35	4.0000	0.0000	0.00000
	UBL	35	4.2571	0.44344	0.07495
Information overload	NBP	35	4.3143	0.75815	0.12815
	UBL	35	4.4000	0.49705	0.08402
Lack of understanding of KM	NBP	35	4.1429	0.69209	0.11698
	UBL	35	4.1429	0.60112	0.10161
Number of clients	NBP	35	4.1429	0.35504	0.06001
	UBL	35	4.1143	0.32280	0.05456
Improve worker efficiency	NBP	35	4.0286	0.16903	0.02857
	UBL	35	4.2857	.45835	0.07748
Knowledge sharing vertically	NBP	35	3.9143	0.28403	0.04801
	UBL	35	3.9143	0.28403	0.04801
Responsibility of the knowledge officer	NBP	35	3.0571	0.99832	0.16875
	UBL	35	3.9143	0.37349	0.06313
Knowledge sharing horizontally	NBP	35	4.0000	0.000000	0.00000
	UBL	35	4.0571	0.23550	0.03981
New knowledge creation	NBP	35	3.9429	0.23550	0.03981
	UBL	35	4.2000	0.40584	0.06860

Table 10: T-Test of hypothesis 1

Independent Samples Test

		Leven's Test for Equality of Variances		t-test for Equality of Means						
		F	Sig.	t	df	Sig. (2-tailed)	Mean Difference	Std. Error Difference	95% Confidence Interval of the Difference	
									Lower	Upper
KM under different name	Equal variances assumed	10.203	0.002	-1.506	68	.137	-.11429	.07591	-.26576	.3719
	Equal variances not assumed			-1.506	56.549	.138	-.11429	.07591	-.26632	.03775
Responsibility of managers	Equal variances assumed	110.118	.000	-3.431	68	.001	-.25714	.07495	-.40671	-.10757
	Equal variances not assumed			-3.431	34.000	.002	-.25714	.07495	-.40947	-.10482
Information overload	Equal variances assumed	.599	.442	-.599	68	.578	-0.8571	.15324	-.39149	.22006
	Equal variances not assumed			-.599	58.670	.578	-.08571	.15324	-.39238	.22095
Lack of understanding of KM	Equal variances assumed	.174	.678	.000	68	1.000	.0000	.15495	-.30920	.30920
	Equal variances not assumed			.000	66.963	1.000	.0000	.15495	-.30931	.30931
Number of clients	Equal variances assumed	.499	.482	.352	68	.726	.02857	.08111	-.13328	.19042
	Equal variances not assumed			.352	67.393	.726	.02857	.08111	-.13330	.19045
Improve worker efficiency	Equal variances assumed	68.026	.000	-3.114	68	.003	-.25714	.08258	-.42192	-.09237
	Equal variances not assumed			-3.114	43.080	.003	-.25714	.08258	-.42366	-.09062
Knowledge sharing vertically	Equal variances assumed	.000	1.000	.000	68	1.000	.00000	0.06790	-.13548	.13548
	Equal variances not assumed			.000	68.000	1.000	.00000	.06790	-.13548	.13548
Responsibility of the knowledge officer	Equal variances assumed	162.038	.000	-4.757	68	.000	-.85714	.18017	-1.21667	-.4762
	Equal variances not assumed			-4.575	43.335	.000	-.85714	.18017	-1.22041	-.49388
Knowledge sharing horizontally	Equal variances assumed	9.340	.003	-1.435	68	.156	-.05714	.03981	-.13658	.02229
	Equal variances not assumed			-1.435	34.000	.160	-.05714	.03981	-.13804	.02376
New knowledge creation	Equal variances assumed	15.337	.000	-3.242	68	.002	-25714	.07931	-.41541	-.09888
	Equal variances not assumed			-3.242	54.566	.002	-.25714	.07931	-.41612	-.09817

Hypothesis 2 (H2) is, KM usage in employees of private banks will be higher than employees of public bank. Statistically can be represented as: KM $Usage_{UBL}$ > KM $Usage_{NBP}$

Table 11 presents the descriptive statistics of hypothesis 2. For hypothesis 2 the variable KM usage of both banks is selected which has 10 different measures related to KM usage. The descriptive statistics presents the summary of whole data. 6 out of 10 measurement items have higher mean values in UBL than NBP, 3 measurement items have same mean values whereas 1 measurement item has less mean value in UBL than NBP. On the basis of higher mean values in more measurement items, we can state that KM usage is higher in private bank (UBL) than public bank (NBP) which proves our hypothesis 2 valid.

Table 12 shows the T test (Statistical formula of T-test is t = [(x1 - x2) - d] / SE) of hypothesis 2, which is used to test whether there is a significant differences between the means of two groups. Since we are using a 95% confidence, alpha = 0.05, therefore if $p < 0.05$ we reject our hypothesis and accept null hypothesis. Under the "t-test for Equality of Variances" the "Sig." for "Equal variances assumed", 3 out of 10 measurement items have less than 0.05 values, therefore we can say there is a significant difference between the variance of two groups.

Table 11: Descriptive statistics of hypothesis 2

Group Statistics

	ID	N	Mean	Std. Deviation	Std. Error Mean
Value System	NBP	35	2.2286	.42604	.07201
	UBL	35	2.3143	.47101	.07961
Capturing knowledge from competitors	NBP	35	4.0000	.00000 [a]	.00000
	UBL	35	4.0000	.00000 [a]	.00000
Formal training to KM	NBP	35	4.0000	.00000 [a]	.00000
	UBL	35	4.0000	.00000 [a]	.00000
Responsibility of KM unit	NBP	35	2.0286	.16903	.02857
	UBL	35	2.0286	.16903	.02857
Improve knowledge worker retention	NBP	35	2.0286	.38239	.06463
	UBL	35	3.6286	.49024	.08287
Grant resources for external knowledge	NBP	35	3.9714	.16903	.02857
	UBL	35	4.0286	.16903	.02857
Informal training to KM	NBP	35	2.1429	.35504	.06001
	UBL	35	2.1143	.47101	.07961
Transfer of knowledge as a function	NBP	35	2.0286	.16903	.02857
	UBL	35	2.0857	.28403	.04801
Lessons learned	NBP	35	4.0857	.28403	.04801
	UBL	35	4.1143	.32280	.05456
Written KM policy	NBP	35	2.0571	.23550	.03981
	UBL	35	2.9143	.50709	.08571

a. t cannot be computed because the standard deviations of both groups are 0.

Table 12: T-Test of hypothesis 1

Independent Samples Test

		Leven's Test for Equality of Variances		t-test for Equality of Means						
		F	Sig.	t	df	Sig. (2-tailed)	Mean Difference	Std. Error Difference	95% Confidence Interval of the Difference	
									Lower	Upper
Value System	Equal variances assumed	2.556	.115	-.798	68	.427	-.08571	.10735	-.29993	.12850
	Equal variances not assumed			-.798	67.327	.427	-.08571	.10735	-.29997	.08063
Responsibility of KM unit	Equal variances assumed	.000	1.000	.000	68	1.000	.00000	.04041	-.08063	.08063
	Equal variances not assumed			.000	68.000	1.000	.00000	.04041	-.08063	.08063
Improve knowledge worker retention	Equal variances assumed	23.649	.000	-15.225	68	.000	-1.60000	.10509	-1.80971	-1.39029
	Equal variances not assumed			-15.225	64.194	.000	-1.60000	.10509	-1.80993	-1.39007
Grant resources for external knowledge	Equal variances assumed	.000	1.000	-1.414	68	.162	-.05714	.04041	-.13777	.02349
	Equal variances not assumed			-1.414	68.000	.162	-.05714	.04041	-.13777	.02349
Informal training to KM	Equal variances assumed	.127	.723	.287	68	.775	.02857	.09970	-.17038	.22752
	Equal variances not assumed			.287	63.207	.775	.02857	.09970	-.17065	.22779
Transfer of knowledge as a function	Equal variances assumed	4.439	.039	-1.023	68	.310	-.05714	.05587	-.16863	.05434
	Equal variances not assumed			-1.023	55.399	.311	-.05714	.05587	-.16909	.05480
Lessons learned	Equal variances assumed	623	.433	-.393	68	.695	-.02857	.07268	-.17360	.11646
	Equal variances not assumed			-.393	66.916	.695	-.02857	.07268	-.17364	.11650
Written KM policy	Equal variances assumed	7.424	.008	-9.070	68	.000	-.85714	.09451	-1.04573	-.66856
	Equal variances not assumed			-9.070	48.015	.000	-.85714	.09451	-1.04716	-.66713

5. CONCLUSION AND RECOMMENDATION

After measuring the level of KM awareness, the conclusion of first objective says that KM awareness is higher in private bank of Pakistani banking sector than public bank. Second objective was to measure the level of knowledge management usage in public and private banks from Pakistani banking sector. After measuring the level of KM usage, the conclusion of second objective says that KM usage is higher in private bank of Pakistani banking sector than public bank. There are two hypotheses in the study; first hypothesis is "KM awareness in employees of public banks will be lesser than employees of private banks" which is proven valid with the help of descriptive and inferential statistics. Second hypothesis is "KM usage in employees of private banks will be higher than employees of public banks" which is also proven valid with the help of descriptive and inferential statistics.

It is recommended that further research can be done on the barriers which occur in implementing KM strategies and research can also be done on knowledge transfer process and procedures. The knowledge in the minds of employees, information/knowledge system, and organizational culture are the most valuable assets. It is also recommended that organizations now track the level of knowledge growth and analyze the rate of change in KM implementation. In addition, KM awareness and usage studies should be performed on a wider sample of same banks, to better measure the true level.

ACKNOWLEDGEMENTS

Authors pay thanks to the employees of National Bank of Pakistan (NBP) and United Bank Limited (UBL) for co-operating well in survey.

REFERENCES

[1] Thomas, J. C., Kellogg, W. A., and Erickson, T., "The knowledge management puzzle: Human and social factors in knowledge management". IBM, Vol. 40, No. 4, pp. 165-172, 2001.

[2] Barquin, R.C., "What is knowledge management? Knowledge and innovation": Journal of the KMCI, Vol. 2, pp. 127-132, 2001.

[3] http://lnweb18.worldbank.org/ "Building knowledge economies", World Bank., 2002, (Accessed: 2009, January)

[4] Jeff Angus and Jeetu Patel, an Information Week article, March 16, 1998. http://www.informationweek.com/

[5] Manfred Bornemann," An Illustrated Guide to Knowledge Management", 2003, http://www.wm-forum.org/

[6] Davenport, Thomas H and Prusak, Laurence "Working Knowledge: How Organizations Manage What They Know", Harvard Business School Press, ISBN 0-87584-655-6, 178 pages, 2002.

[7] Davenport, Thomas H and Prusak, Laurence "Working Knowledge: How Organizations Manage What They Know", Harvard Business School Press, ISBN 0-87584-655-6, 178 pages, 2000.

[8] Oxford Dictionary and Thesaurus, http://www.askoxford.com/

[9] Polanyi, Michael, "The Tacit Dimension", Anchor Books, Double Day and Company, Garden City, New York, 1967

[10] http://en.wikipedia.org/wiki/Knowledge_management11] Mike Burk http://www.tfhrc.gov

AFFINE TRANSFORM RESILIENT ROBUST WATERMARKING TECHNIQUE FOR MEDICAL IMAGES BASED ON IMAGE NORMALIZATION AND SALIENT FEATURE POINTS

Nisar Ahmed Memon *, Asad Ali**, Shaukat Iqbal***

ABSTRACT

To address the issue of copyright protection of medical images in case of affine transformations, we propose a robust image watermarking method using an integrated solution involving moment normalization and salient feature based watermarking in Discrete Cosine Transform domain. First, a new watermarking method based on second generation watermarking concept is proposed. We use salient regions based on Harris feature point detector for watermark embedding and detection process. Second regarding the affine transform attacks, we do not rely upon the normalized disks. We instead use whole image normalization which is resilient to almost all affine transformations such as scaling, translation, rotation, shearing and flipping. The robustness of the approach is verified using both simple and composite affine transformations.

1. INTRODUCTION

The availability of the off-the-shelf image processing software tools in the market has made it easy for hackers and pirates to copy and manipulate the copyrighted digital content. This has increased the threat for digital content owners who use the open networks like internet for transferring their digital assets [4]. New challenges have arisen in the context of easier access and distribution of digital data, especially regarding protection of sensitive medical information. Complementary and/or alternative solutions are nowadays requested in order to confront a number of issues relating to healthcare information management [5]. Millions of medical images are produced daily in radiological departments of the hospitals around the globe. These images are valuable source for both the medical researchers and physicians. This has stimulated continuous expansion and evolution of digital libraries in Medicine, which provide fast and efficient data retrieval from numerous databases in order to foster the creation of new knowledge for medical researchers, and to promote best practice in medical treatment planning for physicians [9]. Consequently information access from these medical image databases raise number of issues that must be addressed, especially those related to security. When a medical practitioner or researcher receives a medical image he/she must be ensured that the image is issued from right source. Thus source authentication of medical images is very important matter relating to health management and distribution [9]. One solution for the protection of medical images is digital image watermarking techniques [6, 8, 9, 10, 24]. The idea is to embed information about the copyright owner into the host image to prevent parties from claiming to be the rightful owners of the data. The watermarks used for that purpose are supposed to be very robust against various attacks intended to remove the watermark [28]. A large number of medical image watermarking techniques [1, 16, 20, 22, 27] been reported in literature for addressing the issue of copyright protection and authentication of medical images. These works are robust to image noise, compression, and spatial filtering, but show severe problems when undergo affine transformations [15]. Affine transformations are also called geometrical distortions and include rotation, scaling translation, cropping, shearing, and projective transformation.

Based on above considerations, we present a blind robust watermarking scheme which is resilient to affine transformations and does not require original image for detection process. The scheme conforms to the strict specifications regarding health data handling by addressing the issue of copyright protection of medical images and preserving their quality and diagnostic value. The scheme embeds the watermark information in the image outside the regions which are important for describes the affine transform resilient watermarking

* Department of Computer Systems Engineering, QUEST, Nawabshah, Pakistan, Email: nisar@quest.edu.pk
** Institute of Industrial Science, University of Tokyo, Tokyo, Japan, Email: asad@iis.u-tokyo.ac.jp
*** Theoretical Plasma Physics Division, PINSTECH, Nilore, Islamabd, Pakistan, Email:shaukat.iqbal.k@gmail.com

approaches. The Concept of feature based watermarking is explained in Section 4. Section 5 explains the proposed scheme and finally experimental results and discussions are described in Section 6.

2. IMAGE NORMALIZATION

In order to cope with the affine transformations introduced in medical images, the image is first normalized in some standard form having the properties of resisting affine transformations. Transforming the image into its standard form requires defining the normalization parameters that are computed from the geometric moments of the image. Let $f(x, y)$ denotes a digital medical image of size $M \times N$, its geometric moments m_{pq} and central moments μ_{pq} for $p, q = 1, 2, 3,...,n$ are defined as:

$$m_{pq} = \sum_{x=0}^{M-1}\sum_{y=0}^{N-1} x^p y^q f(x, y) \tag{1}$$

and

$$\mu_{pq} = \sum_{x=0}^{M-1}\sum_{y=0}^{N-1} (x-\overline{x})^p (y-\overline{y})^q f(x, y) \tag{2}$$

where

$$\overline{x} = \frac{m_{10}}{m_{00}}, \overline{y} = \frac{m_{01}}{m_{00}}$$

Generally an affine transformed image of input image $f(x,y)$ is defined as $G(x_a,y_a)$, where

$$\begin{bmatrix} x_a \\ y_a \end{bmatrix} = A\begin{bmatrix} x \\ y \end{bmatrix} + d \tag{3}$$

provided that det(A) $\neq$ 0. The Equation 3 can also be written as,

$$\begin{bmatrix} x_a \\ y_b \end{bmatrix} = \begin{bmatrix} a_{11} & a_{12} \\ a_{21} & a_{22} \end{bmatrix}\begin{bmatrix} x \\ y \end{bmatrix} + \begin{bmatrix} d_1 \\ d_2 \end{bmatrix} \tag{4}$$

In Equation 4 the matrix A is composite matrix of different affine transformations and is defined as,

$$\begin{bmatrix} x_a \\ y_b \end{bmatrix} = \begin{bmatrix} \cos\theta & -\sin\theta \\ \sin\theta & \cos\theta \end{bmatrix}\begin{bmatrix} \alpha & 1 \\ 1 & \delta \end{bmatrix}\begin{bmatrix} 1 & \beta \\ \gamma & 1 \end{bmatrix}\begin{bmatrix} x \\ y \end{bmatrix} + \begin{bmatrix} d_1 \\ d_2 \end{bmatrix} \tag{5}$$

In Equation 5, the first three matrices on right hand side are called Rotation, Scaling and Shearing matrices, and term after plus sign is called shift or translation vector. The α, δ, β and γ are called transform parameters and are calculated from the image moments by deriving the following results.

Lemma1

If $G(x, y)$ is an affine transformed image of $f(x, y)$ obtained with affine matrix $\begin{bmatrix} a_{11} & a_{12} \\ a_{21} & a_{22} \end{bmatrix}$ and d=0, the following identities hold:

$$m'_{pq} = \sum_{i=0}^{p}\sum_{j=0}^{q}\binom{p}{i}\binom{q}{j} a_{11}^i a_{12}^{p-i} a_{21}^j a_{22}^{q-j} m_{i+j,p+q-i-j} \tag{6}$$

and

$$\mu'_{pq} = \sum_{i=0}^{p}\sum_{j=0}^{q}\binom{p}{i}\binom{q}{j} a_{11}^i a_{12}^{p-i} a_{21}^j a_{22}^{q-j} \mu_{i+j,p+q-i-j} \tag{7}$$

where m'_{pq}, μ'_{pq} are the moments of $G(x, y)$ and m_{pq}, μ_{pq} are the moments of $f(x, y)$.

In our work we adopt the normalization procedure as proposed in [7]. After calculating the transform parameters, the normalization procedure is applied on input medical image which produces the image in some standard form as shown in Figure 1. This standard form of the image always have the same shape even image undergoes simple or composite affine transformations

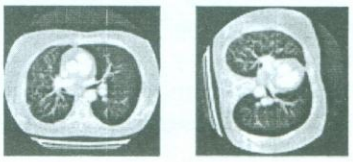

(a) (b)

Figure 1: (a) Original Image (b) Normalized image

3. AFFINE TRANSFORM RESILIENT WATERMARKING APPROACHES

Number of affine transform resilient watermarking approaches is reported in literature. These approaches are roughly divided into four categories:

3.1 INVARIANT DOMAIN-BASED WATERMARKING

In this approach watermarks are embedded and synchronization is maintained in geometric invariant domain. Examples of this type of watermarking are described in [17, 21].

3.2 TEMPLATE-BASED WATERMARKING

In this type of approach additional structured templates are added in frequency domain for identifying geometrical transformations which in turn assisting synchronization. This type of approach is reported in [23].

3.3 MOMENT-BASED WATERMARKING

Geometric moments are employed to normalize the image for maintaining geometric invariance. This type of approach is reported in [2, 3, 12].

3.4 FEATURE-BASED WATERMARKING

In this approach salient regions or object features are utilized for the recovery of geometric attacks. Usually some corner or edge detector such as SIFT, Harris, FAST, SUSAN is used to find the feature points. This approach is reported in [5, 13, 25]. Our proposed method falls in this category.

4. SALIENT FEATURE BASED WATERMARKING

The salient feature-based watermarking is also called content-based image watermarking. This type of watermarking techniques is categorized as second generation watermarking techniques. In this type of watermarking usually feature points are extracted to represent the content of image. Salient points are defined as isolated points in image for which a given saliency function is maximal. The points can be corners or locations of high frequency [26]. In addition points are perceptually significant parts of image and can thus resist various types of common signal processing such as JPEG compression, and geometric distortions. These feature points can also act as marks for (location) synchronization between watermark embedding and detection [25]. In the proposed method we use Harris corner detector [11] as a tool for finding feature points.

5. PROPOSED METHOD

This section describes the proposed method by explaining the embedding and extraction procedures.

5.1 GENERATION OF INVARIANT REGIONS

The proposed method uses Harris feature-based invariant regions to embed the watermark. For this purpose we first normalize the image as described in Section 2 to make the image invariant to rotation, scaling, translation, shearing, and flipping. Harris feature points are then selected from normalized image. In order to detect watermarks without the help of original image, we must look for feature points that are perceptually significant and can resist various image processing operations and desynchronizing attacks. For this purpose we find most stable feature points from a set of detected feature points. For each detected feature point, the search within a circular window whose radius is set to some value say r, is performed. If the detector response R at the feature point achieves local maximum, it is selected as locally most stable point, otherwise it is discarded. Figure 2(a) shows the locally most stable points selected on XRAY medical image. In Figure 2(a), some of the circular windows are overlapping with each other. To obtain non-overlapped patches, the feature point with biggest response say P_{max} in the set of overlapped feature points is chosen and points whose windows overlap with that of P_{max} are then discarded. The procedure for selecting non-overlapped feature points is further discussed in [18]. Figure 2(b) shows the finally selected non-overlapped most stable feature points. It can be observed from Figure 2(b) that some of the stable feature points are lying on the edges of the normalized image. These feature points are vanished when the image is inverse normalized. It is therefore required to discard these feature points too. For this purpose, we use the following procedure. Find the number of black pixels in each circular area, if the number of black pixels is greater than 10% of the total pixels of the circular area it is discarded. Figure 2(c) shows the finally selected feature points used for embedding the watermark.

5.2 BLOCK-BASED EMBEDDING

As mentioned earlier, the proposed method uses feature points for watermark synchronization, therefore

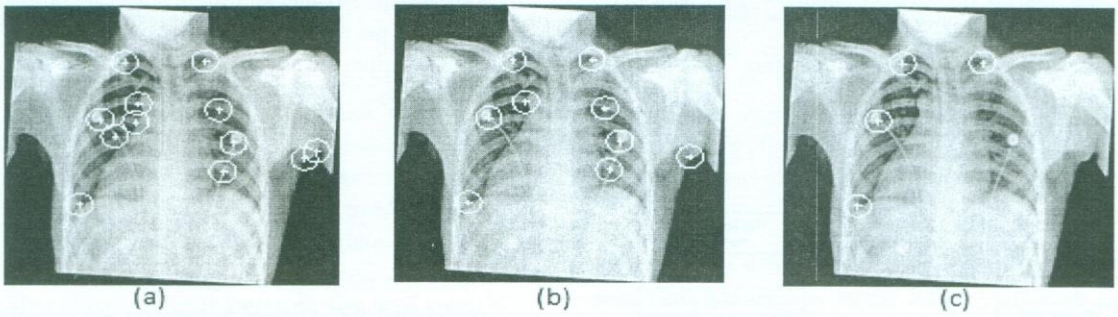

Figure 2: (a) Feature points selected by Harris Corner Detector (b) Non-overlapped Locally most stable points (c) Finally selected feature points

watermark embedding should not affect these feature points. Keeping this point in mind, we propose the block-based DCT-domain embedding instead of full-frame, and leave the middle block of patch without embedding any watermark information. This prevents the neighbouring pixels around the feature point from modification. This helps not only in maintaining the synchronization but also results in accurate recovery of watermark information. Figure 3(a) shows the proposed method of embedding based on block-based embedding in the patch and Figure 3(b) shows the full-frame embedding of patch.

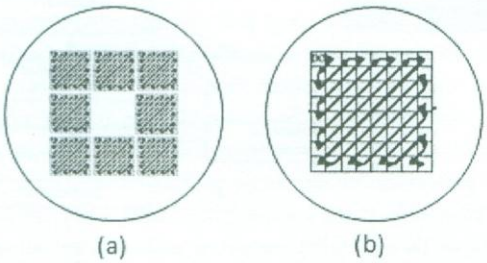

Figure 3: (a) Proposed block-based method of embedding (b) Watermarking embedding method used in [18].

5.3 EMBEDDING PROCEDURE

The block diagram of embedding procedure is shown in Figure 4, and its each step is explained as follows:

1. Normalize the image so that it becomes invariant to affine transformations, as described in Section 2;
2. Apply the Harris corner detector to find the non-overlapped most stable feature points;
3. Extract the rectangular patch from circular region based on each feature point;
4. Divide the rectangular region into nine 8×8 blocks;
5. Divide the watermark into 8 equal parts;
6. Embed each part of the watermark in each block of the patch after transforming it into DCT domain and following the zigzag scan, leaving the middle block unmodified, as shown in Figure 3(a);
7. The embedding is performed by selecting 8 pairs of adjacent coefficients from mid-frequency DCT coefficients in each block;
8. If f_1 and f_2 are DCT coefficients within a pair, and b_i is the watermark bit, then embed the watermark as follows:

   If $b_i = 1$ and $K = f_1 - f_2 < T$, then

   $$f_1^{'} = f_1 + \frac{T-K}{2}$$

   $$f_2^{'} = f_2 - \frac{T-K}{2}$$

   else if $K = f_1 - f_2 > T$, do nothing

   and

   If $b_i = 0$ and $K = f_2 - f_1 < T$, then

   $$f_1^{'} = f_1 - \frac{T-K}{2}$$

   $$f_2^{'} = f_2 + \frac{T-K}{2}$$

   else if $K = f2 - f1 > T$, do nothing;

   Repeat this process for all 8 blocks in rectangular patch;
9. Apply inverse DCT on each block and reconstruct the watermarked rectangular patch;
10. Replace the rectangular patch with the watermarked one in circular region;

11. Finally, replace the original circular region with the watermarked circular region;
12. Repeat steps 4-11 until all feature points are processed.

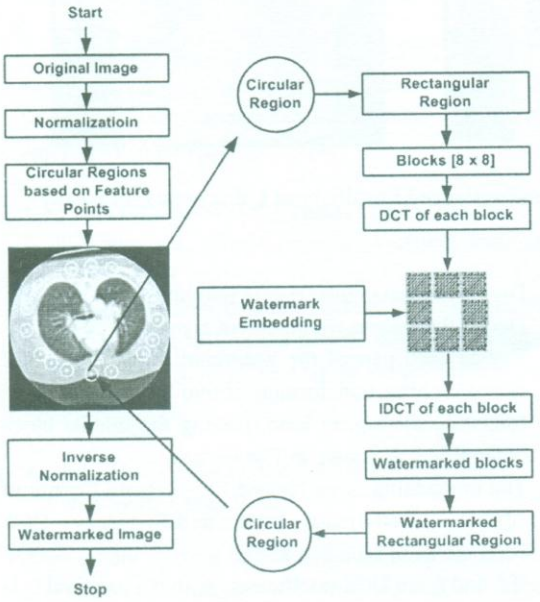

Figure 4: Block diagram of embedding process

5.4 EXTRACTION PROCEDURE

In watermark extraction procedure, first several steps are similar to those of watermark embedding procedure. The block diagram of extraction procedure is shown in Figure 5 and is explained as under:

1. Normalize the image so that it becomes invariant to affine transformations, as described in Section 2;
2. Apply the Harris corner detector to find the non-overlapped most stable feature points;
3. Extract the rectangular patch from circular region based on feature point;
4. Divide the rectangular region into nine 8 × 8 blocks;
5. Extract the watermark information from each block leaving the central block by using the equation;

$$\hat{b}_i = \begin{cases} 1; & f_1' \geq f_2' \\ 0; & f_1' < f_2' \end{cases} \qquad (8)$$

6. Concatenate the watermark information extracted from each block into single watermark $\hat{b}$;
7. Repeat steps 3-6 until all feature points are processed;
8. Calculate the normalized correlation (N_c) to evaluate the similarities between the embedded and extracted watermarks:

$$N_c = \frac{\sum_{i=1}^{n} b(i)\hat{b}(i)}{\sqrt{\sum_{i=1}^{n} b^2(i)}\sqrt{\sum_{i=1}^{n} \hat{b}^2(i)}} \qquad (9)$$

where n is the length of watermark and b and $\hat{b}$ are the original and extracted watermarks respectively;

9. Decide the authenticity of image by considering the maximal N_c value obtained from all the patches.

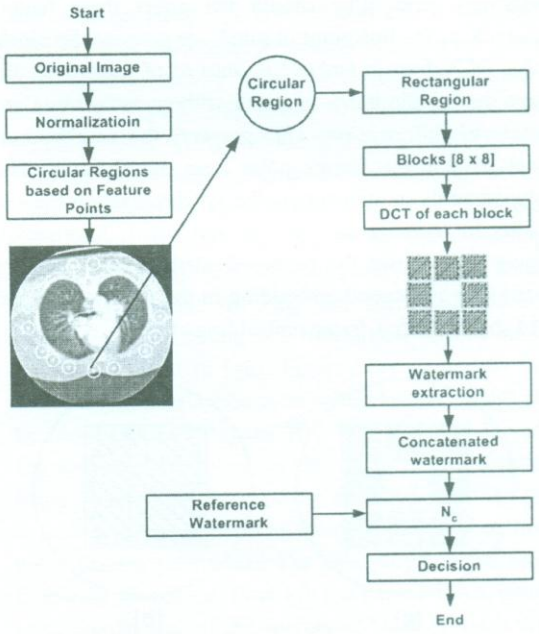

Figure 5: Block diagram of extraction process

6 EXPERIMENTAL RESULTS AND DISCUSSIONS

The concept of affine transform distortions in medical images is new and few works are reported. However, the existing works addressing the issue of the affine transform distortions report results on natural images, we therefore first compare our proposed technique with the existing techniques on standard Lena image and then we report results for medical images.

6.1 RESULTS ON NATURAL IMAGES

In first phase of experiments we apply the proposed algorithm on standard Lena image of size 512 × 512. In order to convey the copyright information in image, a pseudo random binary sequence is generated by using a secret key and this generated sequence is used as watermark. The length of watermark is fixed as 32 bits, which is sufficient for conveying copyright information for a natural image. The distortion introduced in Lena image after watermarking is measured with peak signal to noise ratio (PSNR) and is found 37.07dB. In order to show the robustness of the proposed method a number of geometrical distortions is applied on Lena image. We compare our results with [14] and [18]. The comparative results are shown in Table 1. It can be observed from Table 1, that the proposed method is robust to RST as well composite RST attacks. For rotation attacks our method can tolerate the distortion more than 60 degrees in case of Lena image. The proposed is robust to scaling, even when image is scaled down to more than half of its original size. The method is also robust to composite attacks like rotation followed by scaling, rotation followed by JPEG compression and scaling followed by JPEG compression. In all attacks from S.No. 1 to 28, proposed method performs better than [14] and [18]. This is mainly due to the fact that Lee's scheme embeds the watermark in spatial domain some what like added noise and Li's scheme gives poor response to feature point detector due to embedding on or near to feature point position, whereas the proposed method uses block-based DCT domain watermarking technique for embedding and leaves the block where feature point exists, thus does not allow the modification in feature point as well as in its neighbourhood. We also report the results of horizontal and vertical flipping and number of shearing attacks applied on x-axis, y-axis and combined attacks like rotation followed by shearing, scaling followed by shearing, translation followed by shearing and shearing followed by JPEG compression with different quality factors. These attacks are listed from S.No. 29 to 49 in Table 1. Most of the attacks have N_c greater than 0.7 which reveals the robustness of the proposed method.

6.2 RESULTS ON MEDICAL IMAGES

In the second phase we test the proposed scheme on medical images. The proposed algorithm is not directly applied on medical images due to the following reasons:

1. Medical images are composed of region of interest (ROI) and region of non-interest (RONI). ROI is important for physician for making diagnosis, so its integrity must be maintained during watermark embedding process.
2. The amount of distortion should be as minimum as possible

Keeping these points in mind, we propose to embed the watermark information in the RONI only. Also in the proposed method a small amount of distortion is introduced due interpolation process when we normalize the image before embedding and inverse normalize after embedding. In order to get better tradeoff between the imperceptibility and robustness we use watermark of small size. For medical images we also have used the watermark of same size as for natural images i.e 32 bits. In order to avoid the watermark embedding in region of interest, we take the arbitrary shape for isolating the ROI from RONI. For CT scan images we separate the actual lung parenchyma by segmenting the CT scan image into ROI and RONI. We adopt the segmentation technique proposed in [19] for this purpose. While for other medical images we take the arbitrary circular window with radius equal to 100 pixels. For finding the locally most stable feature points after normalizing the medical image we apply the Harris corner detector with following two methods.

(a) DFS method

In this method we find feature points by applying the Harris Corner detector first and then for maintaining the integrity of ROI, we discard the feature points lying in ROI. This method gives better results for images like MRI, Ultrasound and XRAY. However in case of CT scan images it was found that detector was unable to find feature points on most of the CT Scan images, thus makes the DFS method unsuitable for watermarking the CT scan images. This was due to the fact that the CT scan image contains the lung parenchyma which is highly textured region with clear edges. As Harris corner detector mostly finds corners as feature points, so most of the feature points found were concentrated in region of interest. And as per requirement of RONI embedding if we discard all the feature points lying in ROI, all feature points found by DFS method are vanished from input CT scan image and

ISSN 1665-8607

results in no feature point selected for further embedding. This scenario is shown in Figure 6. In order to overcome this deficiency we proceed for the second method.

(b) SFD method

In this method we isolate the ROI first and then apply the Harris Corner detector for extracting feature points. The

Table 1: Watermark robustness to geometric attacks on Lena Image

S.No.	Type of attack	Normalized Correlation		
		Lee et al. [14]	Li et al. [18]	Proposed
01.	R(1)	0.643	1.000	1.000
02.	R(5)	0.641	1.000	1.000
03.	R(10)	0.600	1.000	1.000
04.	R(15)	0.536	1.000	1.000
05.	R(30)	0.514	0.734	1.000
06.	R(45)	-	-	1.000
07.	R(60)	-	-	1.000
08.	R(75)	-	-	0.930
09.	S(0.2)	-	-	0.516
10.	S(0.3)	-	-	0.645
11.	S(0.5)	-	0.672	0.819
12.	S(0.7)	0.472	1.000	1.000
13.	S(0.9)	0.605	1.000	1.000
14.	S(1.1)	0.606	1.000	1.000
15.	S(1.3)	0.594	1.000	1.000
16.	S(1.5)	0.524	1.000	1.000
17.	S(1.7)	-	-	1.000
18.	S(1.9)	-	-	1.000
19.	T(5)	-	1.000	1.000
20.	T(10)	-	0.820	1.000
21.	R(5)+S(0.8)	-	0.953	0.968
22.	R(10)+S(0.8)	-	0.984	1.000
23.	R(15)+S(0.8)	-	0.969	1.000
24.	R(30)+S(0.8)	-	0.719	0.829
25.	R(10)+JPEG(80)	-	0.953	0.966
26.	R(30)+JPEG(80)	-	0.734	0.876
27.	S(0.8)+JPEG(80)	-	0.891	0.903
28.	S(1.5)+JPEG(80)	-	1.000	1.000
29.	ShX(0.1)	-	-	0.968
30.	ShY(0.1)	-	-	0.933
31.	ShX(0.1)+ShY(0.1)	-	-	0.966
32.	Horizontal Flip	-	-	1.000
33.	Vertical Flip	-	-	1.000
34.	R(10)+ShX(0.1)+ShY(0.1)	-	-	0.852
35.	R(20)+ShX(0.1)+ShY(0.1)	-	-	0.733
36.	R(30)+ShX(0.1)+ShY(0.1)	-	-	0.750
37.	R(10)+ShX(0.2)+ShY(0.2)	-	-	0.859
38.	R(20)+ShX(0.3)+ShY(0.3)	-	-	0.791
39.	S(0.8)+ShX(0.1)+ShY(0.1)	-	-	0.968
40.	S(0.8)+ShX(0.2)+ShY(0.2)	-	-	0.828
41.	S(0.8)+ShX(0.3)+ShY(0.3)	-	-	0.791
42.	T(5)+ShX(0.1)+ShY(0.1)	-	-	0.966
43.	T(10)+ShX(0.2)+ShY(0.2)	-	-	0.870
44.	T(15)+ShX(0.3)+ShY(0.3)	-	-	0.808
45.	ShX(0.1)+JPEG(80)	-	-	0.933
46.	ShY(0.1)+JPEG(80)	-	-	0.866
47.	ShX(0.1)+ShY(0.1)+JPEG(80)	-	-	0.939
48.	ShX(0.2)+ShY(0.2)+JPEG(60)	-	-	0.791
49.	ShX(0.4)+ShY(0.4)+JPEG(90)	-	-	0.800

"-" = Not reported by author, "R" = Rotation, "S" = Scaling, "T" = Translation
"ShX"= Shear on X-axis, "ShY"=Shear on Y-axis

ISSN 1665-8607

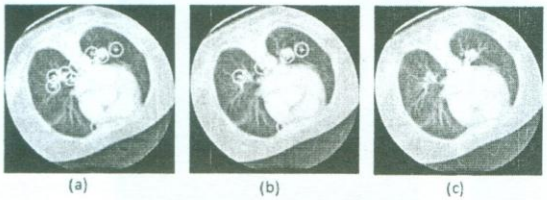

Figure 6: (a) Feature points selected by corner detector on normalized CT scan image (b) Non-overlapped most stable feature points (c) No feature point selected for embedding watermark information.

detailed procedure is defined as under:

1. Mark the logical boundary on the normalized image for isolating ROI;
2. Extend the logical boundary by distance of r, where r is the radius of the circular window;
3. Crop the area bounded by the extended boundary;
4. This will clearly produce the black hole in the image, thus force the detector to find the feature points around the ROI.

The complete cycle of SFD method is depicted in Figure 7.

Figure 8 shows the finally selected feature points for all CT, MRI, Ultrasound and XRAY image by using both DFS and SFD methods. Column 1 in Figure 8 shows the original images, column 2 shows the feature points selected by DFS method and column 3 shows the feature points selected by SFD method. Table 2 shows the number of feature points selected by each method. It can be observed from Table 2, that second method SFD works well and gives assurance of finding sufficient number of feature points for watermarking, every time when it is applied on medical image. We tested the proposed method on CT, MRI, Ultrasound and XRAY images. All images are of size 512 × 512. The value of radius used for circular window is taken as 20 pixels. The watermark length is 32 bits.

Table 2: Locally most stable feature points found by two methods

Image	DFS Method	SFD Method
CT	0	11
MRI	6	13
Ultrasound	7	8
XRAY	4	14

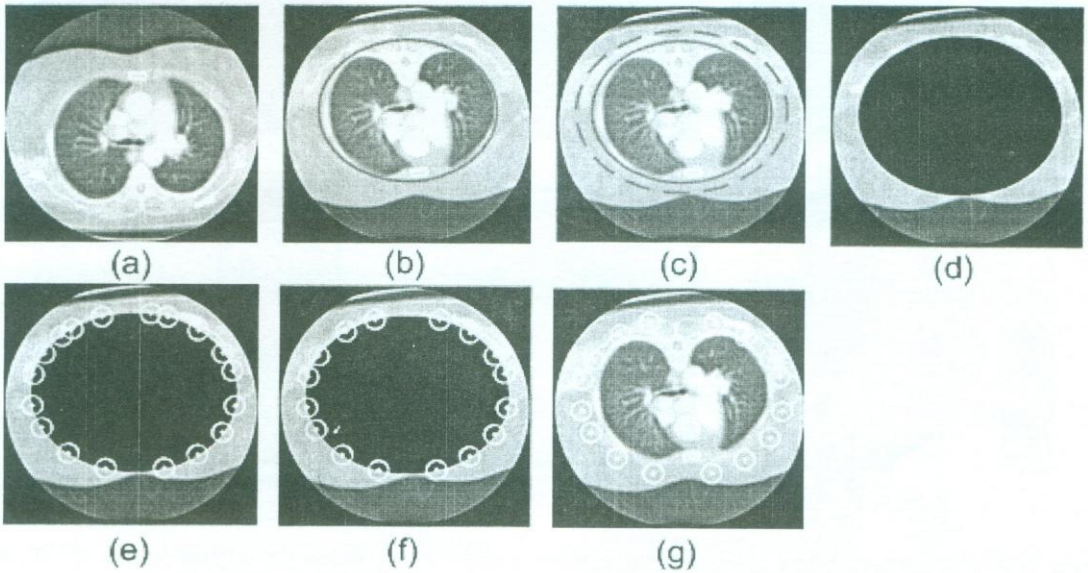

Figure 7: Complete cycle of SFD method: (a) Original image (b) Normalized image with ROI isolated (c) Logical boundary extended (d) Area cropped bounded by extended logical boundary (e) Feature points selected by corner detector (f) Non overlapped feature points selected (g) Finally selected feature points shown on normalized CT scan image

ISSN 1665-8607

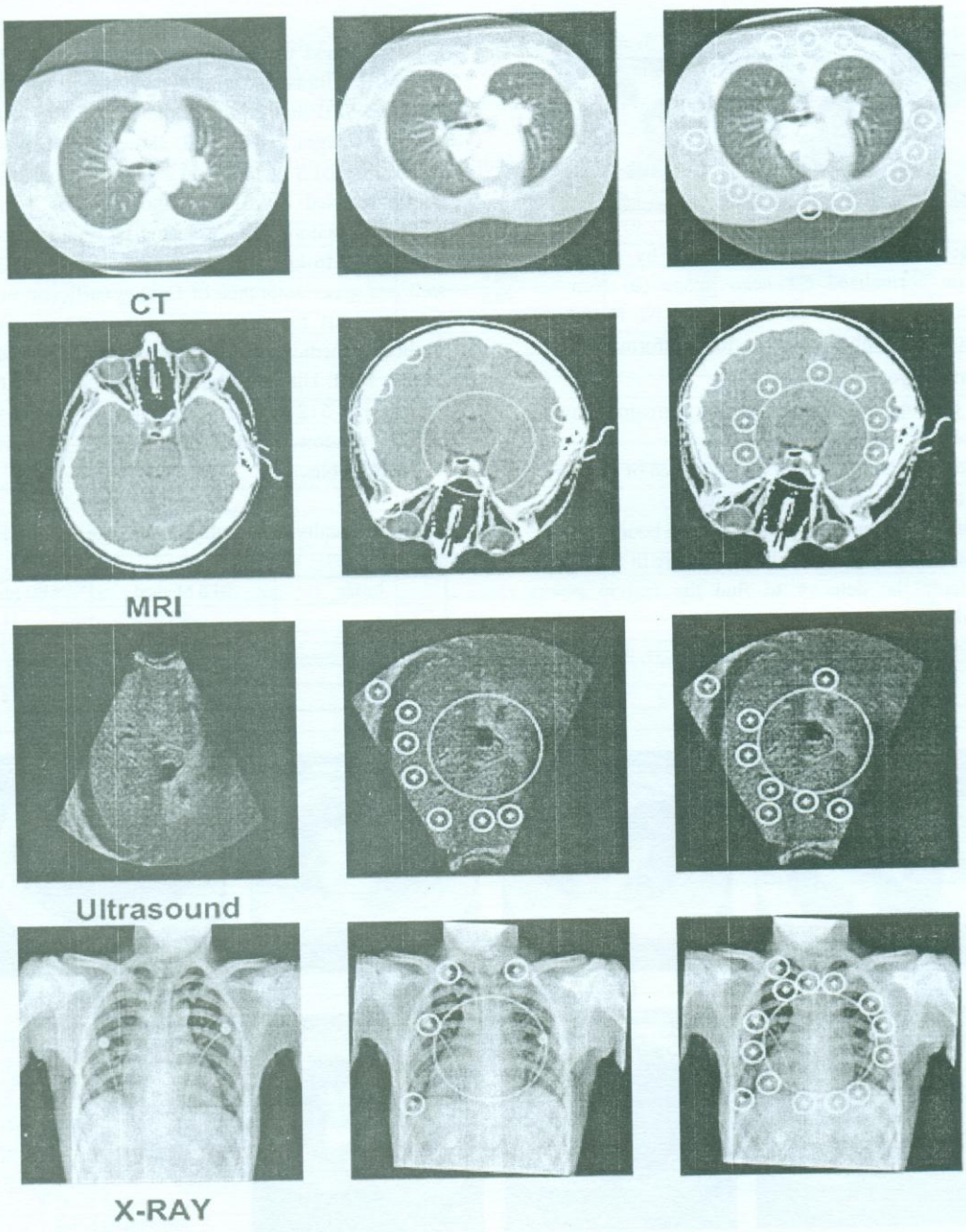

Figure 8: Finally selected feature points by two methods. Column No. 1 shows the original images of CT, MRI, Ultrasound, and XRAY, column No. 2 shows the feature points selected by DFS method and column No. 3 shows the SFD method

The original, watermarked and residual (difference between original and watermarked images) are shown in Figure 9. The distortion introduced in images is measured by using the Peak Signal to Noise Ratio (PSNR). Table 3 shows the values of PSNR for each image. All images have PSNR values greater than 40dB which shows the good imperceptibility of watermarked images.

Table 3: Distortion introduced in cover images after watermarking in terms of PSNR(dB)

Image	PSNR(dB)
CT	45.4449
MRI	47.7396
Ultrasound	49.0673
XRAY	45.9373

In order to show the robustness of the proposed scheme against affine transformations a number of attacks is performed using simple and composite attacks on CT, MRI, Ultrasound and X-ray medical images. The results are tabulated in Table 4 and Table 5. It can be observed from Table 4, that when no attack is performed, the proposed method extracts the watermark accurately. For rotation attacks up to 30 degree most values of normalized correlation are higher than 0.8. The proposed method is robust to scaling, even when the watermarked image is scaled down to 75% of the original size. When the image is zoomed in, most similarities are equal to one or near to 1. This is because when the image is zoomed in, little information is lost. The scheme is also robust to translation attacks. The proposed method is also robust to shearing attacks. From Table 5, we can observe that if we shear the image either on x-axis or y-axis or on both x-axis and y-axis simultaneously up to shearing ratio of 0.1, most similarities are equal to 1. The scheme is also robust to combined attacks such as rotation plus shearing, scaling plus shearing, translation plus shearing.

7. CONCLUSIONS

A blind robust watermarking method based on feature point watermarking and image normalization technique is proposed for the copyright of medical images. Several invariant regions are extracted for conveying the copyright information. Initially image is normalized to make it invariant against geometric distortions and other affine transformations. The circular regions are then extracted from the normalized image. On the basis of invariant regions robust watermarking technique is designed. DCT domain is used for both watermark embedding and extraction. The proposed method address the issue of affine transformations such as shearing, flipping and composite attacks of all affine transformations beside the basic transformations like rotation, scaling and translation.

Table 4: Watermark robustness to geometric attacks medical images

Type of attack	Normalized Correlation			
	CT	MRI	Ultrasound	XRAY
No attack	1.0000	1.0000	1.0000	1.0000
R(1)	1.0000	0.9682	1.0000	0.9682
R(5)	1.0000	0.9682	1.0000	1.0000
R(10)	1.0000	0.9393	0.9682	1.0000
R(15)	1.0000	0.9037	0.9333	0.9333
R(30)	1.0000	0.8391	0.8593	0.8120
R(45)	0.8767	0.7591	0.6000	0.7112
R(60)	0.7912	0.6888	0.4900	0.5010
R(75)	0.6901	0.4521	0.3912	0.4210
S(0.2)	0.5809	0.5333	0.3330	0.5331
S(0.3)	0.5923	0.6055	0.4667	0.5333
S(0.5)	0.7333	0.6516	0.6888	0.6888
S(0.7)	0.9393	0.8767	0.8281	0.7912
S(0.9)	1.0000	0.9837	0.9500	1.0000
S(1.1)	1.0000	1.0000	0.9801	1.0000
S(1.3)	1.0000	1.0000	1.0000	1.0000
S(1.5)	0.8281	0.9333	0.9333	0.9661
S(1.7)	0.8787	0.8520	0.7201	0.7515
S(1.9)	0.7912	0.7000	0.6624	0.7100
T(5)	1.0000	1.0000	1.0000	1.0000
T(10)	1.0000	1.0000	1.0000	1.0000
R(5)+S(0.8)	0.9393	0.8971	0.8767	0.9661
R(10)+S(0.8)	1.0000	0.9837	0.9037	0.7591
R(15)+S(0.8)	0.9661	0.9129	0.9393	0.9682
R(30)+S(0.8)	0.8767	0.8667	0.8391	0.7810

Table 5: Watermark robustness to geometric attacks on medical images

Type of attack	Normalized Correlation			
	CT	MRI	Ultrasound	XRAY
R(10)+JPEG(80)	0.7515	0.7100	0.6445	0.6086
R(30)+JPEG(80)	0.7303	0.5923	0.6351	0.5196
S(0.8)+JPEG(80)	0.6055	0.6694	0.6211	0.5023
S(1.5)+JPEG(80)	1.0000	0.8520	0.9666	0.9682
ShX(0.1)	0.9333	1.0000	0.9393	1.0000
ShY(0.1)	1.0000	1.0000	1.0000	1.0000
ShX(0.1)+ShY(0.1)	1.0000	1.0000	0.9393	1.0000
Vertical Flip	1.0000	1.0000	1.0000	1.0000
Horizontal Flip	1.0000	1.0000	1.0000	1.0000
R(10)+ShX(0.1)+ShY(0.1)	0.9682	0.9333	0.8767	1.0000
R(20)+ShX(0.1)+ShY(0.1)	1.0000	1.0000	1.0000	1.0000
R(30)+ShX(0.1)+ShY(0.1)	1.0000	1.0000	1.0000	1.0000
R(10)+ShX(0.2)+ShY(0.2)	1.0000	1.0000	0.9037	1.0000
R(20)+ShX(0.3)+ShY(0.3)	0.8667	0.8885	0.8767	1.0000
S(0.8)+ShX(0.1)+ShY(0.1)	0.9682	0.9682	0.8971	0.9682
S(0.8)+ShX(0.2)+ShY(0.2)	0.9227	0.8767	0.6901	0.8520
S(0.8)+ShX(0.3)+ShY(0.3)	0.8667	0.7108	0.7303	0.5505
T(5)+ShX(0.1)+ShY(0.1)	1.0000	1.0000	0.9393	1.0000
T(10)+ShX(0.2)+ShY(0.2)	0.9037	1.0000	0.8767	0.8971
T(15)+ShX(0.3)+ShY(0.3)	1.0000	0.9037	0.8944	0.8293
ShX(0.1)+JPEG(80)	0.7006	0.7100	0.6761	0.7515
ShY(0.1)+JPEG(80)	0.7100	0.6888	0.5774	0.7100
ShX(0.1)+ShY(0.1)+JPEG(80)	0.7156	0.6761	0.6262	0.6000
ShX(0.2)+ShY(0.2)+JPEG(80)	0.6901	0.5164	0.4146	0.5022
ShX(0.3)+ShY(0.3)+JPEG(80)	0.5899	0.5477	0.5477	0.5636

ISSN 1665-8607

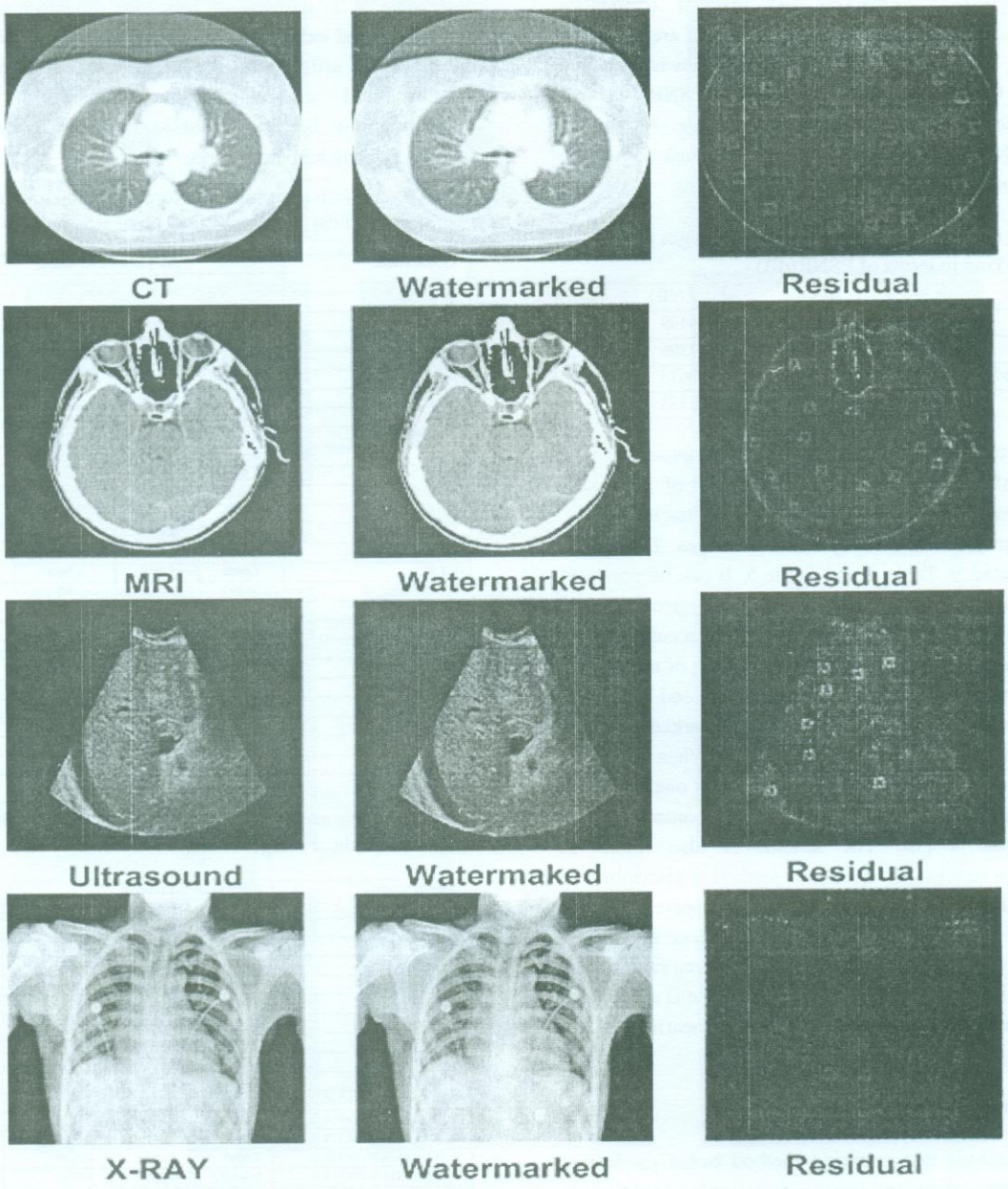

Figure 9: From Left to Right: column 1 shows the original images, column 2 shows the watermarked images and column 3 shows the residual images (difference between original and watermarked images).

In order to maintain the integrity of ROI of a medical image, ROI is avoided from embedding the watermark. The proposed method finds the place in the medical data management, where geometric distortions are of great concern. However one limitation of the proposed method is the introduction of small amount of distortions produced due to interpolation errors when we normalize and inverse normalize the image during watermarking process. Though ROI is prevented during the watermark embedding process, the interpolation errors still can cause distortion in the ROI. One method for avoiding such type of distortions can be the introduction of the improved methods of interpolation which can avoid the interpolation errors in ROI and result in better quality of watermarked image.

ACKNOWLEDGEMENT

Authors are very grateful to Ghulam Ishq Khan Instiute of Engineering Sciences and Technology, Topi, Swabi, Pakistan for providing resources and environment for carrying out this research. Image databases were provided by AGA Khan Medical University Hospital, Karachi, Pakistan. This work was supported by Quaid-e-Awam University of Engineering, Science and Technology, Nawabshah, Sindh, Pakistan under Inland Scholarship programme.

REFERENCES

[1] U. R. Achariya, P. S. Bhat, S. Kumar, L. C. Min, "Transmission and storage of medical images with patient information", Journal of Computers in Biology and Medicine, vol. 33, pp. 303-310, 2003.

[2] M. Alghoniomy, A. H. Twefik, "Image watermarking by moment invariants", Proceedings IEEE International Conference on Image Processing, vol. 2, pp. 73-76, 2000.

[3] M. Alghoniomy, A. H. Twefik, "Geometric invariance in image watermarking", IEEE Transactions on Image Processing, vol. 13, No. 2, pp. 145-153, 2004.

[4] P. Bas, J.-M. Chassery, B. Macq, "Geometrically invariant watermarking using feature points", IEEE Transactions on Image Processing, vol 11, pp. 1014-1028, 2002.

[5] S. Battacharjee, M. Kutter, "Compression tolerance image authentication", Proceedings of IEEE International Conference on Image Processing, vol. 1, pp. 435-439, 1998.

[6] R. R. Colin, C. F. Uribe, J.-A. M. Villanueva, "Robust watermarking scheme applied to radiological medical images", IEICE Transactions on Information and Systems (Letter), vol. E91-D, No.3. , 2008.

[7] P. Dong, J. G. Brankov, N. P. Galatsanos, Y. Yang, F. Davoine, "Digital watermarking robust to geometric distortions", IEEE Transactions on Image Processing 14(12), 2140-2150. 2005.

[8] A. Giakoumaki, S. Pavlopoulos, D. Koutsouris, "Multiple digital watermarking applied to medical imaging", Proceedings of the IEEE 27th Annual Conference on Engineering in Medicine and Biology, Shanghai, China, vol. 4, pp. 3444-3447. 2005.

[9] A. Giakoumaki, S. Pavlopoulos, D. Koutsouris, "Multiple image watermarking applied to health information management", IEEE Transactions on Information Technology in Biomedicine, vol. 10, No. 4, pp. 722-732, 2004.

[10] G. Goatrieux, J. Montagner, H. Juang, C. Roux, "Mixed reversible and RONI watermarking for medical image reliability protection", Proceedings of IEEE 29th Annual Conference of EMBS, Cite Internationale, Lyon, France, vol. 27, pp. 5654-5657. 2007.

[11] C. Harris, M. Stephens, "A combined corner and edge detector", Proceedings of the Fourth Alvey Vision Conference, Manchester, UK, pp. 147-151, 1998.

[12] H. S. Kim, H. K. Lee, 2003. Invariant image watermarking using zernike moements. IEEE Transactions on Circuits and Systems for Video Technology 13(8), 766-775, 2003.

[13] M. Kutter, S. K. Battacharjee, T. Ebrahimi, "Towards second generation watermarking schemes", Proceedings of IEEE Conference on Image Processing, vol. 1, pp. 320-323, 1999.

[14] H.-Y. Lee, H. Kim, H.-K. Lee, "Robust image watermarking using local invariant features", Optical Engineering, vol. 45, No. 3, pp. 1-11, 2006.

[15] H.-Y. Lee, J.-T. Kim, H.-K. Lee, Y.-H, Suh, "Content-based synchronization using the local invariant feature for robust watermarking", Proceedings of C.H. Lim and M. Yung(Eds.),WISA 2004, Springer LNCS 3325, pp. 122-134. 2004.

[16] M. Li, R. Poovendran, S. Narayanan, "Protecting patient privacy against unauthorized release of medical images in a group communication environment", Journal of Computerized Medical Imaging and Graphics, vol. 29, pp. 367-383, 2005.

[17] C. Y. Lin, M. Wu, T. A. Bloom, I, J. Cox, M. L. Miller, Y. M. Lui, "Rotation, scale and translation resilient watermarking of images", IEEE Transactions on Image Processing, vol. 10, No. 5, pp. 767-782, 2001.

[18] L.-D. Li, B.-L. Guo, L. Guo, "Rotation, scaling and translation invariant image watermarking using feature points", The Journal of China Universities of Posts and Telecommunications, vol. 15, No. 2, pp. 82-87, 2008.

[19] N. A. Memon, A. M. Mirza, S. A. M. Gilani, "Segmentation of lungs from CT scan images for early diagnosis of lung cancer", Proceedings of 2006 Enformatika XIV International Conference, Prague, Czech Republic, vol. 14, pp. 228-233, 2006.

[20] H. Munch, E. Engelmann, A. Schroeter, H. P. Meinzer, "Web-based Distribution of radiological images from PACS to EPR", International Congress Series, vol. 1256, pp. 73-879, 2003.

[21] J. J. K. O'Ruanaidh, T. Pun, "Rotation, scale and translation invariant spread spectrum digital image watermarking", Signal Processing, vol. 66, No. 3, pp. 303-317, 1998.

[22] G.-T. Oh, Y.-B. Lee, S.-J. Yeom,, "Security mechanism for medical image information on PACS using invisible watermark", Proceedings of M. Dayde etl al. (Eds) VECPAR 2004, Springer LNCS, vol. 3402, pp. 315-324. , 2005.

[23] S. Pereira, T. Pun, "Robust template matching for affine resilient image watermarks", IEEE Transactions on Image Processing 9(6), 1123-1129, 2000.

[24] F. Y. Shih, Y.-T. Wu, "Robust watermarking and compression for medical images based on genetic algorithms", Information Sciences Elsevier, vol. 175, pp. 200-216. 2005.

[25] C. W. Tang, H. M. Hang, "A feature based robust digital image watermarking scheme", IEEE Transactions on Signal Processing, vol. 51, No. 4, pp. 950-959, 2003.

[26] C. Wu, R. Cathey, "Digital image watermarking: A comparative overview of several digital watermarking schemes", available www.csam.iit.edu/cs549/cs549/presentation report.pdf, 2002.

[27] J. H. K. Wu, R.-F. Chang, C.-J. Chen, C.-L. Wang, T.-H. Kuo, W. K. Moon, R. Chen, "Tamper detection and recovery for medical images using near lossless information hiding techniques", Journal of Digital Imaging, vol. 21, No. 1, pp. 59-76, 2008.

[28] D. Zheng, Y. Liu, J. Zhao, A. E. Saddik, "A survey of RST invariant image watermarking algorithms", ACM Computing Surveys, vol. 39, No. 2, Article 5, 2007.

FRAUNHOFER DIFFRACTION COMPUTATION OF HOLOGRAMS FOR FICTITIOUS OBJECTS

Abdul Fattah Chandio*, Attaullah Khawaja**, Abdul Sattar Jamali***

ABSTRACT

When a hologram of non-existing object is desired one can compute it mathematically. Such type of holograms are known as computer generated holograms. In this paper such type of holography presented with an experiment of ordinary photographic recording arrangements. The objective of this work is to design computer generated hologram of a fictitious object and coding of that hologram in computer language, finally plotting of that hologram on a paper. Then reconstruction of that object is done from computer generated printed hologram by use of ordinary photographic arrangements. The fictitious objects selected for this work were horizontal lines, vertical lines and the letters comprising of my name FATTAH the coding of this program has been done in MATLAB.

Key Words: Holography, Diffraction, Optical Fourier Transform, CGH

1. INTRODUCTION

Images and photographs are since long in use for identification and location of objects. Photography was introduced after the invention of optical lens. Photograph provides in-depth study of an area; indicates the presence of objects of interest in that area and their location. Images from satellite depict weather changes, agriculture growth, geological and global actions. Special images may contain additional scientific information including object spectral characteristics, velocity, temperature, etc. Hologram is a record of the interaction of two beams of coherent light which are mutually correlated in the form of microscopic pattern of interference fringes. One beam is reference and other one is object beam, the process of fabrication of hologram is known as holography. An ordinary hologram is produced by recording the interference pattern, which is caused by an object wave and a reference wave On this principle Dennis Gabor became the first to record the object wave and name it as hologram in 1948 [1]. But when a hologram is desired of an object, which does not exist physically but is known in mathematical terms, one can compute the hologram. The simulated hologram is drawn by high resolution plotting machine and subsequently photographically reduced in size. This type of hologram is known as computer generated hologram [2,3]. These holograms are Fourier transform holograms. Main advantage of computer generated holography is the fact that the object does not required to exist.

In 1967 another milestone was achieved by introducing a new concept of holography that was "computer generated holography" by A W Lohman and D. P. Paris [2]. Recent advances in three dimensional display technologies have shifted attention to the possibility of true holographic displays [4].

The objectives of this work is construction of computer generated hologram. The class of holography that have been selected for computer simulation is Fourier Transform Holography. The objects used for computer generated holography are horizontal line, vertical line, and the word **FATTAH**. These objects are made of rectangular apertures.

2. DIFFRACTION THEORY

When a light is obstructed by solid body it will create complex shadow of bright and dark regions and can be viewed by placing and screen on other side of body. The phenomenon is known as diffraction. The effect is general characteristic of wave phenomena occurring whenever a portion of wavefront is obstructed in some way when it is propagating in rectilinear direction. If a region of wavefront is altered in amplitude or phase whether it is done by opaque or transparent obstacle diffraction will occur. The various segments of the wavefront that propagate beyond the obstacle interfere, causing the particular energy density referred to as diffraction pattern [5, 6]. The figure 1 shows the diffraction patterns where

* Dept of Electronics Engineering, QUEST Nawabshah, Email: fattahchandio@yahoo.com
** Dept of Electronics Engineering, NED Karachi, Email: atta_khawaja@yahoo.com
*** Dept of Mechanical Engineering, QUEST Nawabshah, Email: jamali_sattar@yahoo.com

structured fringes represent the density of diffracted waves.

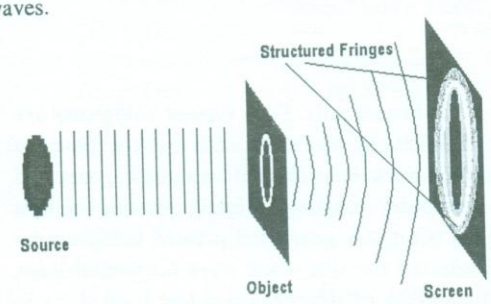

Figure 1: General description of diffraction

3. FRAUNHOFER AND FRESNEL DIFFRACTIONS.

Consider aperture shaped object smaller in size made in solid shield is illuminated by plane waves originated from a point source located at distance ***d***. If image screen is placed at reasonable distance other side of object (i-e aperture sheet) then image of aperture can be observed onto the screen along with some light fringes around the boundaries of aperture. If the image screen is moved farther away from aperture, the image of aperture becomes structured and the fringes become more prominent. This is known as near field or Fresnel diffraction. If the image screen moved farther from the object one stage will come where there will be no change occurs in fringes or image of object only size of image will be changed. Such phenomenon is known as Fraunhofer or far field diffraction.

4. COMPUTER GENERATED HOLOGRAPHY

Hologram is the recording of interference pattern that caused by object beams and a reference beam. Under usual circumstances, the hologram fringes may locally be viewed as arcs of circles, whose radii of curvature are large compared with the local fringe period [7]. Hologram can be desired those objects which does not exist physically but can be deemed in mathematical terms. Such type of holograms is known as computer generated holograms [8]. It is important to mention that computer generated hologram does not need any optical system but can be computed mathematically by using digital computers [9]. Computer generated holograms presented here are binary. In this research creation of hologram is done by computer simulation of Fourier Transform Holography based on Fraunhofer diffraction.

5. DESIGN STEPS COMPUTER GENERATED HOLOGRAPHY

To design computer simulated hologram following steps are adopted.

i. Object specification
ii. Calculation of amplitude and phase of diffracted light from the object.
iii. Sampling of the Fourier Transform
iv. Computation of hologram by calculation of interference between reference beam and object beam
v. Coding Schemes
vi. Plotting of Hologram.

Here in this research objects are considered as assembly of rectangular apertures.

5.1 CALCULATION OF FRAUNHOFER DIFFRACTION PATTERN FOR RECTANGULAR APERTURE

Consider configuration of Rectangular Aperture as shown in Figure 2. Amplitude and phase of light incident at a location X,Y on an image screen located at a distance Z from aperture. The width of aperture is w and height of aperture is h where

$w = x_1 - x_2$ and $h = y_1 - y_2$

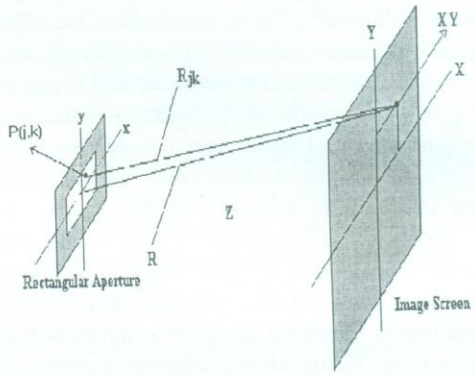

Figure 2: Light distribution by rectangular aperture to an image screen

Consider a point location P(jk) in aperture then R_{jk} the distance between point jk on aperture and X,Y on image screen will be

$$R_{jk} = \sqrt{(X - x_i)^2 + (Y - y_k)^2 + Z^2} \qquad (4\text{-}1)$$

let $R = \sqrt{X^2 + Y^2 + Z^2}$

Then, $R_{jk} = R\sqrt{1 - \frac{2Xx_j}{R^2} + \frac{x_j^2}{R^2} - \frac{2Yy_k}{R^2} + \frac{y_k^2}{R^2}}$

as R>>x_j ,y_k therefore we can neglect the terms x_j^2/R^2 and y_k^2/R^2 therefore

$$R_{jk} = R - \frac{Xx_j}{R} - \frac{Yy_k}{R}$$

Now if we consider the diffraction from whole aperture (X,Y) is E(X,Y) and R_{jk} = R' then we can write

$$E(X,Y) = \int_{y_2}^{y_1}\int_{x_2}^{x_1} ae^{i\frac{2\pi R'}{\lambda}}\,dxdy \qquad (4\text{-}2)$$

substituting the value of R' in Equation (4-2) then

$$E(X,Y) = \int_{y_2}^{y_1}\int_{x_2}^{x_1} ae^{i\frac{2\pi}{\lambda}\left(R-\frac{Xx}{R}-\frac{Yy}{R}\right)}dxdy$$

Or

$$E(X,Y) = ae^{i\frac{2\pi R}{\lambda}}(x_1-x_2)e^{-i\frac{\pi X(x_1+x_2)}{\lambda R}} * \operatorname{sinc}\left(\frac{\pi X(x_1-x_2)}{\lambda R}\right) * (y_1-y_2)e^{-i\frac{\pi Y(y_1+y_2)}{\lambda R}}\operatorname{sinc}\left(\frac{\pi.Y(y_1-y_2)}{\lambda R}\right) \qquad (4\text{-}3)$$

Equation (4-3) is the generalized equation for Fraunhofer diffraction by a rectangular aperture on an image screen located at a distance Z from the aperture.

5.2 INSERTION OF LENS FUNCTION

Fraunhofer diffraction can be achieved when image screen is at infinite distance so theoretically value of Z is infinite to avoid this problem we place a lens between aperture and image screen so that same phenomenon can be achieved by placing image screen at one f distance from lens. By considering Equation (4-1) and solving R_{jk} in the form of parallel distance Z, gives:

$$R_{jk} = \sqrt{X^2 - 2Xx_j + x_j^2 + Y^2 - 2Yy_k + y_k^2 + Z^2}$$
$$= Z\left[1 + \frac{X^2+Y^2}{2Z^2} + \frac{x_j^2+y_k^2}{2Z^2} - \frac{x_jX}{Z^2} - \frac{y_kY}{Z^2}..\right]$$

if we ignore all terms of high powers of xj and y_k which are divided by high power terms of Z and replace 'x_j' by 'x', 'y_k' by .'y' then

$$R_{jk} \cong Z + \frac{X^2+Y^2}{2Z} - \frac{xX+yY}{Z} \qquad (4\text{-}4)$$

now take R_{jk}=R' and substituting 4-4 in Equation (4-2) that is

$$E(X,Y) = \int_{y_2}^{y_1}\int_{x_2}^{x_1} ae^{i\frac{2\pi}{\lambda}\left(Z+\frac{X^2+Y^2}{2Z}-\frac{xX+yY}{Z}\right)}dxdy$$

or

$$E(X,Y) = ae^{i\frac{2\pi}{\lambda}Z\left[1+\frac{X^2+Y^2}{2Z^2}\right]}\int_{y_2}^{y_1}\int_{x_2}^{x_1} e^{i\frac{2\pi}{\lambda}\left[\frac{xX+yY}{Z}\right]}dxdy$$

where as Z>>X, Z>>Y in other words $1>>(X^2+Y^2)/Z^2$ therefore we can write

$$E(X,Y) = ae^{i\frac{2\pi Z}{\lambda}}\int_{y_2}^{y_1}\int_{x_2}^{x_1} e^{-i\frac{2\pi}{\lambda}\left[\frac{xX+yY}{Z}\right]}dxdy \qquad (4\text{-}5)$$

now if we analyse Equation (4-5) we will see that all terms on left hand side of integral signs are constants and will perform a uniform action on all diffracting light waves in image screen so we can eliminate them by one suffix C.

$$E(X,Y) = C\int_{y_2}^{y_1}\int_{x_2}^{x_1} e^{-i\frac{2\pi}{\lambda}\left[\frac{xX+yY}{Z}\right]}dxdy \qquad (4\text{-}6)$$

now if we place a well corrected lens of focal length *f* away from the aperture and image screen is placed at rear focal plane then same phenomenon (ie far field diffraction) will be achieved as shown in Figure 3.

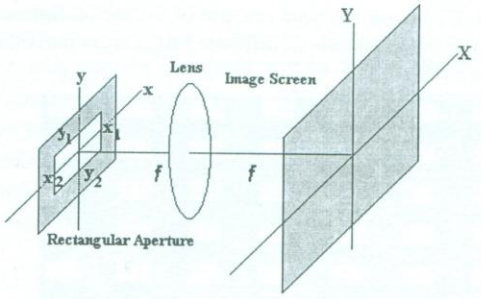

Figure 3: Use of lens in holography

Then Equation (4-6) becomes

$$E(X,Y) = C\int_{y_2}^{y_1}\int_{x_2}^{x_1} e^{-i\frac{2\pi}{\lambda}\left[\frac{xX+yY}{f}\right]}dxdy$$

$$= C(x_1-x_2)(y_1-y_2)e^{-i\frac{\pi(x_1+x_2)X}{f\lambda}}e^{-i\frac{\pi(y_1+y_2)Y}{f\lambda}} * \operatorname{sinc}\left(\frac{\pi(x_1-x_2)X}{f\lambda}\right) * \operatorname{sinc}\left(\frac{\pi(y_1-y_2)Y}{f\lambda}\right)$$

whereas x1-x2=width 'w' of aperture and y1-y2=height 'h' of aperture therefore

$$E(X,Y) = Cwhe^{-i\frac{\pi(x_1+x_2)X}{f\lambda}} e^{-i\frac{\pi(y_1+y_2)Y}{f\lambda}} * \sin c\left(\frac{\pi(x_1-x_2)X}{f\lambda}\right) * \sin c\left(\frac{\pi(y_1-y_2)Y}{f\lambda}\right) \quad (4\text{-}7)$$

Equation (4-7) is the generalized equation for light diffraction from an object of rectangular aperture shaped on an image screen at single point whose location is X,Y in image screen. Whereas f is the focal length of lens which is placed between image screen and object as shown in Figure 3. Equation (4-7) shows the complex amplitude of diffracted light from single rectangle location X,Y in Fourier plane (i-e image screen). Now consider the situation where an object has more then one apertures then the resultant complex amplitude of diffracted light on single point (X,Y) will be the sum of all complex amplitudes of light diffracting from each aperture individual.

Consider Figure 4 where an object comprises of m×n number of rectangle apertures then total light contribution on location XY will be

$$E_T(X,Y) = \sum_m \sum_n E_I(X,Y)$$

Where ET shows the total amount of diffracted light and EI shows the amplitude of diffracted light from individual aperture [10].

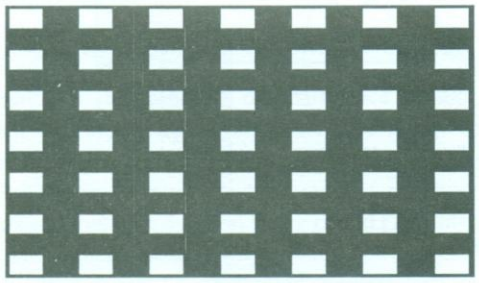

Figure 4: Object consists of m*n number of transparent apertures.

5.3 COMPUTATION OF HOLOGRAM

Hologram is record of an interference pattern formed by superposition of waves, diffracted from an object and the reference wave. A general setting of an ordinary holography is shown in Figure 5 where object is a rectangular aperture. The object wave O is diffracted wave coming from object incident on the image screen and interfere with reference wave R. Then the distribution of intensity recorded on the image screen is given as

$$H = |R+O|^2 .$$

$$H = |R|^2 + |O|^2 + RO^* + OR^* \quad (4\text{-}8)$$

Where

- R = reference wave
- O = object wave
- R^* = conjugate of R
- O^* = conjugate of O

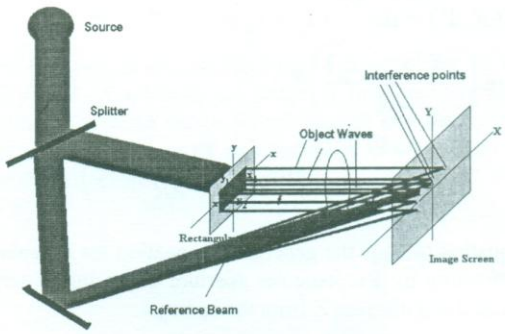

Figure 5: General arrangements for holography

In Equation (4-8) first two terms corresponds the intensities of reference beam and object beams whereas third and fourth terms represents the interference pattern between reference wave and object wave, these are the terms which contains phase and amplitude information of object and reference beam. Our computer program will calculate only third and fourth terms as given below

$$H(X,Y) = RO^* + OR^*$$
$$= 2OR\cos(\varphi_1 - \varphi_2)$$

where φ1 is the phase of object beam and φ2 is the phase of reference beam. In computation of computer simulated hologram the computation of diffracted light distribution on image screen is the object beam. Whereas for reference beam we introduce mathematically a beam of same wavelength as used in calculation of object or diffracted beam.

6. EXPERIMENTS AND RESULTS

For designing and coding of computer generated holograms various mathematically defined objects are used. These objects are Horizontal Line, Vertical Line, Plus Sign, and word FATTAH. These objects are composition of rectangular apertures.

6.1 COMPUTER GENERATED HOLOGRAM OF HORIZONTAL LINE

We take the object as horizontal line in the form of rectangular aperture as shown in Figure 6. To compute the hologram of this object Equation (4-7) is used i.e.

$$E(X,Y) = Cwhe^{-i\frac{\pi(x_1+x_2)X}{f\lambda}} e^{-i\frac{\pi(y_1+y_2)Y}{f\lambda}} * \sin c\left(\frac{\pi(x_1-x_2)X}{f\lambda}\right) * \sin c\left(\frac{\pi(y_1-y_2)Y}{f\lambda}\right)$$

The values of variables are

- **x1 = 1 millimeter**
- **x 2 = -1 mm**
- **y1 = 0.1 mm**
- **y2 = -0.1 mm**
- **f = 4000 mm**
- **$\lambda = 6.2*10^{-4}$ mm**

X,Y are coordinates of Fourier plane where hologram will be computed, so we will select discrete values of X,Y. These discrete values will be in accordance with sampling theorem. For horizontal line hologram two dimensional matrix of 41*41 order will be used to store the phases and amplitudes of hologram with respect to the discrete values of X and Y coordinates. Where X starts from -200 to +200 millimeters with step size of 10 millimeters and Y starts from -200 to +200 millimeters with step size of 10 millimeters in other words sampling rate is 10 millimeters.

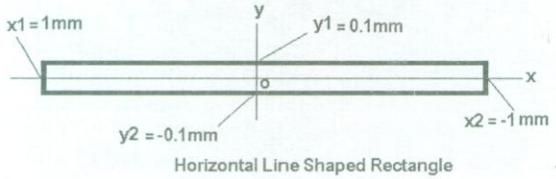

Figure 6: Horizontal line shaped rectangular Aperture

For reference beam we use a plane beam (of same wavelength as that of object beam) of unity magnitude, tilted at 45 degrees with X-Z plane in Fourier plane.

6.2 COMPUTER PROGRAMMING FOR HOLOGRAM.

Computer program used for computation of computer generated hologram is written in MATLAB software. The computer program is divided into five steps:

In first step it will calculate the amplitude and phase of diffracted light wave from object that is Fourier transform of object and store it into a two dimensional array form.
In second step it will calculate the interference pattern between reference plane wave and object wave and store them in a two dimensional array form.

In third step enhancement of amplitude of hologram will be done. The reason for enhancement is such that the amplitudes of higher orders of Fourier transform of object are so small that they are suppressed by the values of amplitudes around the origin of aperture. This difference can be observed by comparing the holograms made with amplitude enhancement shown in Figure 7 and without amplitude enhancement shown in Figures 8. Figure 9 and figure 10 three dimensional plots (surf-plot) with and without amplitude enhancement of holograms.

In fourth step computer program will scale the amplitude of hologram up-to certain limit so that all values below that limit will not be plotted. This is because to have some opaque contrast between two prominent orders in reconstruction

In fifth step the hologram will be graphically plotted on monitor or printed on paper. The graphical representation of hologram is in the form of rectangular opaque dots in such a way that height of dot represents the amplitude of hologram and horizontal offset shift is proportional to the phase of hologram at that discrete location.

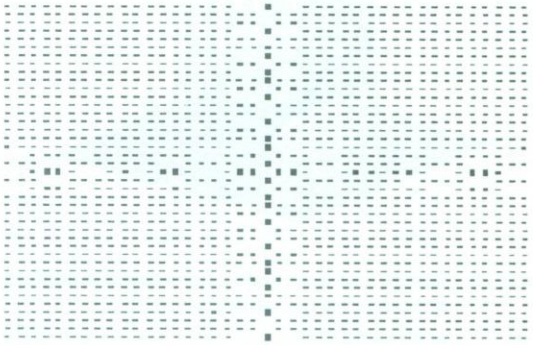

Figure 7: Computer Generated Hologram of Horizontal Line with amplitude enhancement

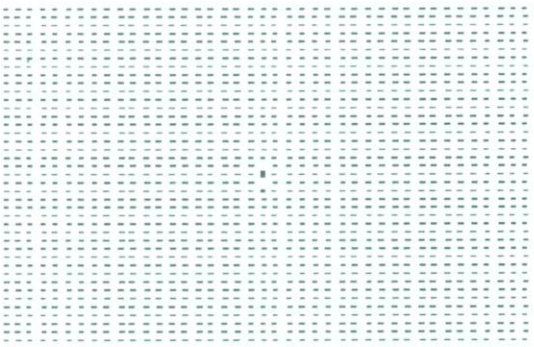

Figure 8: Computer Generated Hologram of Horizontal Line without amplitude enhancement

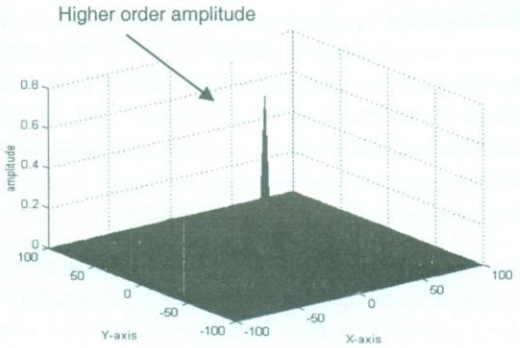

Figure 9: Surf plot of amplitude of computed hologram of horizontal line without amplitude enhancement

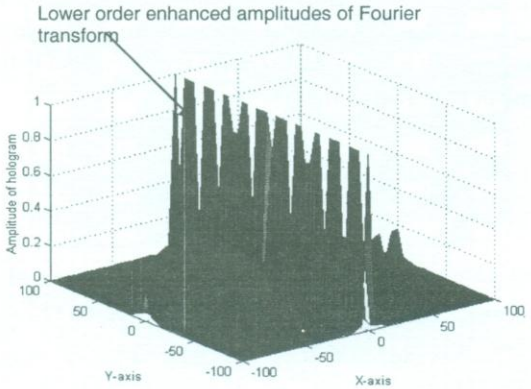

Figure 10: Surf plot of amplitude of computed hologram of horizontal line after amplitude enhancement.

7 CONCLUSION

In this paper computer simulation of Fourier transform holograms, of various objects are designed and constructed. MATLAB has been used for computer programming. Good quality holograms are computed using larger arrays of the data points. The objects that are simulated for computer generated holograms are rectangular apertures, horizontal lines, vertical lines, plus sign and the word FATTAH. Use of rectangular apertures for creation of hologram can also be used to develop 3-D display system for view of 3-D objects [11]. In this work construction of computer generated hologram has been tried on photosensitive film. For this purpose we have used ordinary photographic films and camera. Therefore the recorded holograms were not of good quality. To record good quality high resolution holograms, proper holographic film and the fabrication system is suggested.

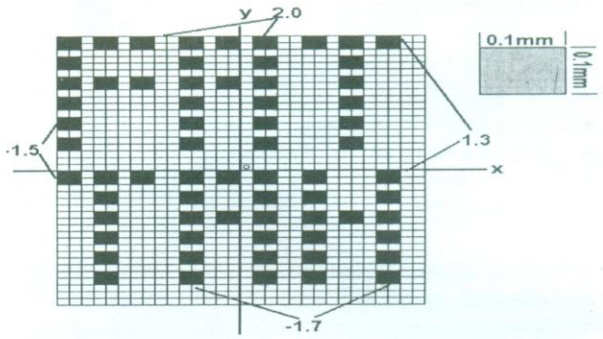

Figure 11: Object 'FATTAH

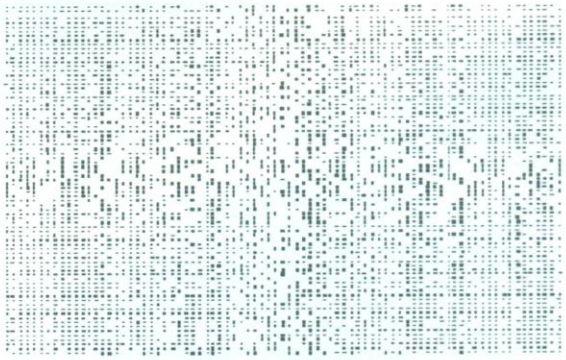

Figure 12: Computer Generated Hologram of object FATTAH

REFERENCES

[1] Gabor D, "A new microscopic principle", Nature, 161, 777,1948.

[2] Lohman A W. and Paris DP, "Binary Fraunhafer holograms generated by computers". Appl Optics, 6, 1739, 1967.

[3] Ichioka Y and Lohman AW, "Interferometric testing of large optical components with circular computer holograms" Appl Optics. 11, 2597, 1972.

[4] Lukas Ahrenberg, Philip Benzie, Marcus Magnor, JohnWatson, "Computer generated holography using parallel commodity graphics hardware" Vol. 14, No. 17 / OPTICS EXPRESS , 2006.

[5] Hecht Eugene, Optics Vol 3 Addision Wesley New York, 1998.

[6] Klein Miles v, Furtak Thomas E, "Optics" Vol 2 John Wiley and Sons, USA, 1986.

[7] Markus Kajanto, Arto Salin, Eero Byckling, Juha Fagerholm, Jussi Heikonen, Jari Turunen, Antti Vasara, and Arto Salin, "Photolithographic fabrication method of computer-generated holographic interferograms" APPLIED OPTICS / Vol. 28, No. 4 / 15 February 1989.

[8] Wyant JC and Bennett V.P, "Using computer generated holograms to test aspheric wavefronts". Appl Optics, 1, 2839, 1972.

[9] G. Schirripa Spagnolo, M. De San, "Computer Generated Hologram for SemiFragile Watermarking with Encrypted Images" International Journal of Signal Processing 4;2 © www.waset.org Spring 2008.

[10] Lukas Ahrenberg, Philip Benzie, Marcus Magnor, JohnWatson, "Computer generated holograms from three dimensional meshes using an analytic light transport model" / Vol. 47, No. 10 / APPLIED OPTICS, 1 April 2008.

[11] Xuewu Xu, Sanjeev Solanki, Xinan Liang, Shuhong Xu, Ridwan Bin Adrian Tanjung, Yuechao Pan,Farzam Farbiz, Baoxi Xu and Tow-Chong Chong, " Computer-Generated Holography for Dynamic Display of 3D Objects with Full Parallax " The International Journal of Virtual Reality, 8(2):33-38,2009.

ISSN 1665-8607

CONTENTS

Volume 9 No. 2 JUL-DEC- 2010

Published by
Directorate of Research & Publication, Quaid-e-Awam University of Engineering, Science & Technology, Nawabshah, District Shaheed Benazir Abad, Shindh-Pakistan.
(Phone#92-244-9370362, Fax # 92-244-9370362) email:jamali_sattar@yahoo.com, editor_rj@quest.edu.pk

Composed & printed by
Samo Computer, Composers & Printers Nawabshah.
Cell: 03337026931 - 03337054383